BUCKLING STRENGTH OF HYPERBOLIC PARABOLOIDS

A thesis submitted in partial fulfilment of the requirements for the degree of

MASTER OF ENGINEERING

in

STRUCTURAL ENGINEERING

By

CHANDRA SHEKHAR SANWAL

DEPARTMENT OF CIVIL ENGINEERING

UNIVERSITY OF ROORKEE

ROORKEE, (INDIA)

1965

CERTIFICATE

CERTIFIED that the dissertation entitled "Buckling Strength of Hyperbolic Paraboloids", which is being submitted by Sri Chandra Shekhar Sanwal, in partial fulfilment for the award of the Degree of Master of Engineering in "Structural Engineering" of the University of Roorkee, Roorkee is a record of students own work carried by him under my supervision and guidance. The matter embodied in the dissertation has not been submitted for the award of any other Degree or Diploma.

This is further to certify that he has worked for a period of seven months from December 15 to July 14 in preparing dissertation for Master of Engineering Degree at the University.

A. Arya

(A.S.Arya)
Assistant Director,
School of Research and Training
in Earthquake Engineering,
University of Roorkee,
Roorkee.

Dated 14 th July,1965.

ACKNOWLEDGEMENTS

The author expresses his deep and sincere gratitude to Dr. A.S.Arya, Assistant Director, School of Research and Training in Earthquake Engineering, University of Roorkee, Roorkee for his constant help and the ablest guidance and feels extremely indebted for the encouragement given by him at every stage.

The author is also thankful to Sri Bishambar Das, Incharge of the Workshop of the Structures Section for his best possible cooperation and appreciates his keen interest in casting the shell model.

CONTENTS

			Page
CHAPTER I-	INTRODUCTION.		
	1.1 Introduction.	...	1-3
	1.2 Object and Scope.	...	4
	1.3 Notations.	...	4-6
CHAPTER II-	THEORY OF BUCKLING.		
	2.1 Historical Review.	...	7-11
	2.2 Theoretical Investigations.	...	11-30
CHAPTER III-	DESIGN OF THE SHELL.		
	3.1 Design Dimensions.	...	31-34
	3.2 Membrane Analysis and Design.	...	35-42
	3.3 Bending Analysis and Design.	...	42-48
	3.4 Design of Edge Beams.	...	48-57
	3.5 Buckling Loads According to Various Theories.	...	58-65
CHAPTER IV-	MODEL TEST.		
	4.1 Choice of Model Scale.	...	66-69
	4.2 Model Design.	...	69-77
	4.3 Buckling Loads (Theoretical) in Model	...	77
	4.4 Constructional Details.	...	78-93
	4.5 Observations and Results.	...	94-109
	4.6 Discussion of Results.	...	109-122
CHAPTER V-	CONCLUSION.		
	5.1 Conclusion.	...	123
	REFERENCES.	...	124-126

CHAPTER I

INTRODUCTION

1.1 Introduction

The hyperbolic paraboloid shells have become very popular all over the world on account of their pleasing appearance and ease of construction. This shell roof has been made popular by the interesting examples of Felix Candella (13) and others. Some very bold and aesthetically pleasing structures have been designed making use of the excellant architectural possibilities of this type of membrane shell. The umbrella type shell is so well known now. The formwork becomes even simpler than those for cylindrical shells because of the peculiar geometrical property of the hyperbolic paraboloid that it can be generated by the translation of a straight line so that each end travels along another straight line. The two straight lines are contained in two parallel planes but are not at the same time in a common plane and therefore the entire form work can be made out of straight boards or planks although the shell surface itself is doubly curved and of negative gaussian curvature.

Furthermore, we obtain an economical use of the construction materials. At the same time, the shell has a simple structural action. By relying on form or shape for strength than on mass, the double curvature enables the loads to be transferred to supports almost entirely by direct forces so that most of the material in the cross-section of the shell is uniformly stressed. Economy in the construction and ease in design of hyperbolic paraboloids allow the architect to depart from the conventional practice of forcing all structures to conform to networks of linear members confined to three perpendicular planes and to make imaginative use of the many graceful

Furthermore, we obtain an economical use of the construction materials. At the same time, the shell has a simple structural action. By relying on form or shape for strength than on mass, the double curvature enables the loads to be transferred to supports almost entirely by direct forces so that most of the material in the cross-section of the shell is uniformly stressed. Economy in the construction and ease in design of hyperbolic paraboloids allow the architect to depart from the conventional practice of forcing all structures to conform to networks of linear members confined to three perpendicular planes and to make imaginative use of the many graceful shapes that may be developed.

As various research workers have noted and also experiences of field engineers have shown, the danger of failures of the thin membrane shells is mainly due to buckling. Nicolas Esquillon(10) has commented,

> " In our opinion, failures caused by shear or buckling are the only dangers in a thin shell roof. These failures are more dangerous because no outward symptoms precede their occurrence, failure is almost instantaneous with the appearance of cracking (shear) or a first light fold (buckling)."

Also as Salvadori (12) comments

> " .... The shell thickness is never determined by membrane stresses, but by stresses due to bending, temperature and buckling."

At present the knowledge on the buckling of shells is scant. Most available information is regarding the cylindrical shells only. It is known that doubly curved shells are more stable against buckling than cylindrical ones because of the surfaces being non-developable. The anti-clastic surfaces must be more so due to the curvatures of opposite nature in two directions, one supporting the other in resisting the buckling as compared to the synclastic shells.

The analysis and design of hyperbolic paraboloid shells themselves are still under a stage of research and experiments. Various theories have been proposed from time to time, but they are all quite complicated even with several simplifying assumptions and none could be well established so far. The buckling phenomenon could hardly be substantially applied to these types of shells so far and much research work remains to be done before the buckling strength of anti-clastic surfaces could be predicted.

1.2 Object and Scope.

The object of this thesis is to study the mode of failure of a R.C. hyperbolic paraboloid and correlate the various theories of buckling available predicting the buckling load with the observations made from the experiment.

A simple hyperbolic paraboloid shell has been designed by membrane theory and edge perturbances are provided for according to the empirical relations given by Vreedenburgh(16). The original shell dimensions are 112'x112'(In plan)centre to centre of supports and 4" thickness with two diagonally opposite corners raised by 20 ft. and 58.3 ft respectively with respect to the other two, which are at the same level. A geometrically similar reinforced concrete model reduced in the ratio of 9.33 has been tested till failure occurred.

1.3 Notations

The following notations have been used unless otherwise mentioned:

a,b	Sides of the shell in plan
a_1,b_1	Widths of the beams along X and Y-directions.
D	Flexural Rigidity of the shell.

E	Young's Modulus of Elasticity.
h	Rise of the shell.
I_a, I_b	Moments of Inertia of the Beams In X and Y-Directions.
k_1, k_2	Principal Curvatures.
N_x	Force per unit length in x-direction on the projected element.
N_y	Force per unit length in y-direction on the projected element.
N_{xy}	Shear on the projected element.
p_{cr}	Critical load uniformly distributed per unit area.
p_o, q	Uniformly distributed load in vertical i.e. Z- direction over shell surface.
p_v	Load per unit area of projected surface.
R	Radius of curvature.
S_x	Force per unit length in the actual shell element along x-axis.
S_y	Force per unit length in the actual shell element along y-axis.
S_{xy}	Shear per unit length on actual shell element.

t	Thickness of the shell.
U_x, U_y, w	Displacements in X, Y and Z-directions.
U	Potential energy.
V	Strain Energy.
xx, yy, zz	Axes of x, y and z.
X, Y, Z	Coordinates of any point.
α	Buckling Coefficient.
ν	Poisson's Ratio.
τ	Shearing Stress.
$\epsilon_x, \epsilon_y, \epsilon_z$	Strains in X, Y and Z- directions.
λ	Characteristic length.

CHAPTER -II

THEORY OF BUCKLING.

2.1. Historical Review.

Zoelly in 1915 gave the following formula for the critical load per unit area of the surface of a spherical shell to cause buckling which was based on Wansleben's theory (1)

$$p_{cr} = \frac{Et^2}{R^2} \cdot \frac{2}{\sqrt{3(1-\nu^2)}}$$

Where t is the thickness and R the radius of curvature the shell and ν, E are the Poisson's ratio and Young's modulus of elasticity respectively for the material.

From this formula it can be seen that the buckling load increases that is to say the danger of buckling decreases as the radius of curvature becomes small. In other words the stability increases as the curvature decreases. Further, the danger of buckling can be substantially reduced by increasing the thickness of the shell.

However, the results according to the formula did not tally with experimental observations and in due course as a result of many observations the formula was given the form:

$$p_{cr} = \propto . \frac{Et^2}{R^2},$$ where $\propto$ is buckling coefficient.

Since then the investigators have been attempting to find out a suitable value of $\propto$, though they are very few in number.

Probably Csonka(6) was the first person to suggest a buckling formula for the doubly curved shells in 1958 in the form

$$p_{cr} = \propto . \frac{Et^2}{R_1 R_2}$$

i.e. the term R^2 for the spherical shells was replaced by $R_1 R_2$ the product of the two radii of curvature for the shells of double curvature. The formula is found to be suitable for synclastic shells but whether it will be applicable as such to the negative gauss curvature shells also remains to be explored.

Further it remains to be decided whether the form of the expression must be the same or a more involved one has to be used. As will be seen later the expressions obtained theoretically for hyperbolic paraboloid shells are quite different, they involve the rise to span ratio of the shell and the flexural rigidites, Since the buckling certainly depends upon the shallowness or depth of the shells, atleast the factor 'h' i.e. rise of the shell must be significantly represented in the expression.

H. Schmidt (4) of Dresden performed tests to determine the value of α for doubly curved shells in general. In order to determine the buckling factor α eight aluminium translation shell models having a circular generatrix were loaded until they buckled by pneumatic load evenly distributed on the whole shell surface. Following the results of his experiments the buckling factor takes the value of 0.320 for practical dimensioning of the shells. α = 0.20 is suggested in case of shells, which can be built with relatively greater accuracy of dimensions e.g. metals and plastics. In case of shells built with lesser accuracy e.g. R.C. shells α = 0.15 is recommended. Regarding factor of safety for concrete shells, the comment of (5) P.W. Abeles, however, is important. " .... it seems not to be appropriate to ignore buckling for R.C. and rely solely upon the high factor of safety for R.C. It is, therefore, suggested that research should be carried out to determine the factor for R.C. combined with appropriate E-value so as to become independent from guessing these coefficients based on tests of steel or aluminium."

This shows the lack of knowledge and little work done on the reinforced concrete shells.

There is no record of any R.C. anti-clastic shell tested for buckling so far. Even in case of synclastic shells such experiments are very few in number. Only experiments conducted on buckling of such R.C. shells seem to have been made by E. Torroja (4) who obtained 0.09 as the value of the factor α.

P. Csonka(6) observed the failure of an actual spheroidal (elliptical paraboloid) R.C. shell (built in 1950 and deformations observed in 1954). The shell built by concrete behaved satisfactorily for a normal snow load condition, but the paraboloid buckled two years after construction when it was subjected to an exceptional snow load. He found $\alpha = 0.062$ with some numerical approximations. Allowing a factor of 20 percent to be still safer he suggested $\alpha = 0.05$.

The value is only one third as compared to Schmidt's factor $\alpha = 0.15$. Thus the vast deviation makes these investigations by tests on R.C. shells all the more necessary so as to affect economical designs in future.

However, if the factor α is taken 0.05 for anticlastic shells their designs may be too conservative since the buckling strength of anticlastic shells is likely to be higher. Of course, for concrete shells one has to be careful specially on account of the phenomena like shrinkage, possible crack formation and creep strains leading to delayed buckling.

The collapse of two hyperbolic paraboloids is reported in the U.S.A. One (24) of these was a reinforced concrete shell 70'x70' of the inverted umbrella type, which collapsed 5 months after construction. The other hyperbolic paraboloid (25) made of laminated wood collapsed at the Seattle world fair several days after the false work had been removed. The shell had a span of 80 feet and rise of 60 feet. The precise causes of these collapses are not known. It is suspected that the failure may have occurred because of creep buckling since the collapses did not occur immediately after removing the form work.

Hence, the need of detailed investigation and testing programme can not be over-emphasised and till that is done, great caution and care in the design of large hyperbolic paraboloid shells of reinforced concrete has to be taken.

2.2 Theoretical Investigations.

It is not an easy matter to determine theoretically the stability of shells, particularly when, apart from buckling phenomenon, second order buckling (oil-canning) is to be taken into account. The latter phenomenon consists of the shell suddenly adopting a new position of equilibrium involving displacements of finite magnitude. The conventional theory, which assumes only infinitesimally small deformations is no longer applicable and must be replaced by a second order theory.

Vreedenburgh (16) states further,

" As regards the danger of second order buckling, which is more serious than the danger of buckling, it seems to us that the hyperbolic paraboloidal shell will be less vulnerable, owing to the saddle form, than the spherical shell. Although this has not yet been proved theoretically, our conjecture is nevertheless confined to same extent by the very high stability of hyper shells, as obtained in the model tests on the Philips Pavilion".

The few attempts for obtaining an expression for the buckling load (uniformly distributed over the shell surface) will now briefly be described.

Eric Reissner in his paper (7) "On Some Aspects of the Theory of Thin Elastic Shells" has utilised the equations of statics. Systematic omission of all but the first terms in the expressions in powers of shell rise furnishes a system of equations suitable for the analysis of shallow membranes. This has been shown to be a special case of general shallow-shell theory based on the statement of Marguerre (8) in his general theory for shallow shells, which considers bending action as well as linear effects.

The use of general shell theory is illustrated with the help of two basic problems of the hyperbolic paraboloid shell under the influence of its own weight. The first problem concerns the possible buckling of such a shell. The second problem however considers the edge effects.

Anthony Ralston(9) also started with the same equation of a hyperbolic paraboloid and assumptions as Reissner and obtained the same differential equations. A numerical solution was attempted and curves between the load coefficient; a function of the uniformly distributed load and the ratio of thickness to rise were plotted for square hyperbolic paraboloids. However, the curves do not enable us in generalising the result as is discussed later.

Dayaratnam and Gerstle(17) have attacked the problem by means of energy procedure.

According to the membrane theory, hyperbolic paraboloid shells under uniform vertical loading are subject to uniform shear stress in the plane of the shell. At the edges of such shells these shear stresses are transferred to the supporting edge members as uniformly applied axial loads which may lead to the buckling of these members and this possibility has to be considered in the design of the structure. In the past an approximate buckling load was obtained by considering the edge member isolated from the shell and calculating its buckling load under uniformly applied axial loads(18). Since this approach neglects all interaction between shell and edge beam, it will at least be a conservative lower bound.

The authors in their paper have attacked the buckling problem by means of an energy method. An expression for the potential energy of shell is established, an appropriate series expression is assumed for the deflected shape, which satisfies compatibility between shell and edge members. It is determined by minimisation of the potential energy that the behaviour is of the nature of a beam-column in which the deformation increases non-linearly with increasing load. The critical value of the membrane shear stress (corresponding to non-unique deformations) is then found by equating the determinant of the characteristic equation to zero. Only shallow shells have been assumed.

Curves have been plotted to indicate the influence of the various parameters on the buckling strength of square shells. The buckling loads thus established are compared with to those obtained by E. Reissner(7).

2.3. Buckling of H.P.Shell (Use of General Shallow Shell Theory)

The shell has the mid-surface equation as

$$Z = h. \frac{x}{a} . \frac{y}{b}$$

It is assumed that the shell is acted upon by uniformly distributed load in the z-direction only, $q_z = p_o$. The edges x = o, a and y = o, b are supposed to have moment-free support and the edge stiffening members are rigid in the direction of their axes and have negligible bending resistance in planes tangent to the shell. It is found after simplification that for $\frac{t}{h} \ll 1$, where t is the thickness and h is the rise of the shell, the shell "crinkles" into waves in the direction of the existing compression. The value at which crinkling takes place is obtained as

$$p_{cr} = \frac{2E}{\sqrt{3(1-\nu^2)}} \cdot \frac{t^2 h^2}{a^2 b^2}$$

Comparing it with the Plate (Stability) formula,

$$p_{cr} = K. \frac{2E}{1-\nu^2} . \frac{b}{a} \left(\frac{t}{b} \right)^3 ,$$

It is seen that the Plate Formula depends on the various dimensions of the shell which differ from the shell formula. The Shell Theory formula shows a more pronounced dependence on shell rise 'h' and a less pronounced dependence on the shell thickness 't' than the Plate Theory formula.

Replacing the critical load by critical shearing stress produced by the load p_{cr} we have

$$\tau_{cr} = \frac{N_{xy}}{t} = \frac{p_{cr}}{t} . \frac{ab}{2h}$$

$$= \frac{E}{\sqrt{3(1-\nu^2)}} . \frac{th}{ab}$$

Again comparing this buckling formula with the corresponding formula for simply supported plates

$$\tau_{cr} = K. \left(\frac{a}{b} \right) . \frac{E}{1-\nu^2} \left(\frac{t}{b} \right)^2$$

We find that except for a difference in the numerical coefficients the shell formula differs from the plate formula in that the thickness square factor is replaced by the product of shell thickness and rise.

Numerical Solutions and P-β curves

The differential equations are of the form:

$$\nabla^2 \nabla^2 \phi = Eh \frac{2h}{ab} \cdot \frac{\partial^2 w}{\partial x \partial y}$$

$$D \nabla^2 \nabla^2 w = - \frac{2h}{ab} \cdot \frac{\partial^2 \phi}{\partial x \partial y} + p_o \frac{ab}{h} \cdot \frac{\partial^2 w}{\partial x \partial y}$$

ϕ is a stress function and other quantities are same as referred earlier. A numerical solution has been attempted. The deflected shape is assumed in the following form as done earlier by Reissner:

$$w = \sum_{m=1}^{\infty} \sum_{n=1}^{\infty} A_{mn} \cdot \sin \frac{m \pi x}{a} \sin \frac{n \pi y}{b}$$

Calculations were made for the case of square shape i.e. a = b and convergence of the solution was observed in the solutions obtained by taking the number of terms in the above expression for w from first two to eighteen. Expressing a load coefficient

$$P = \frac{po \sqrt{12(1-\nu^2)}}{4E \beta^2} \cdot \frac{b^4}{h^4}$$

where $\beta = \frac{t}{h}$ (thickness to rise ratio), the curves between P and β were plotted, whose shapes are given below (Figure No.1)

P- β CURVES FOR H.P. SHELLS

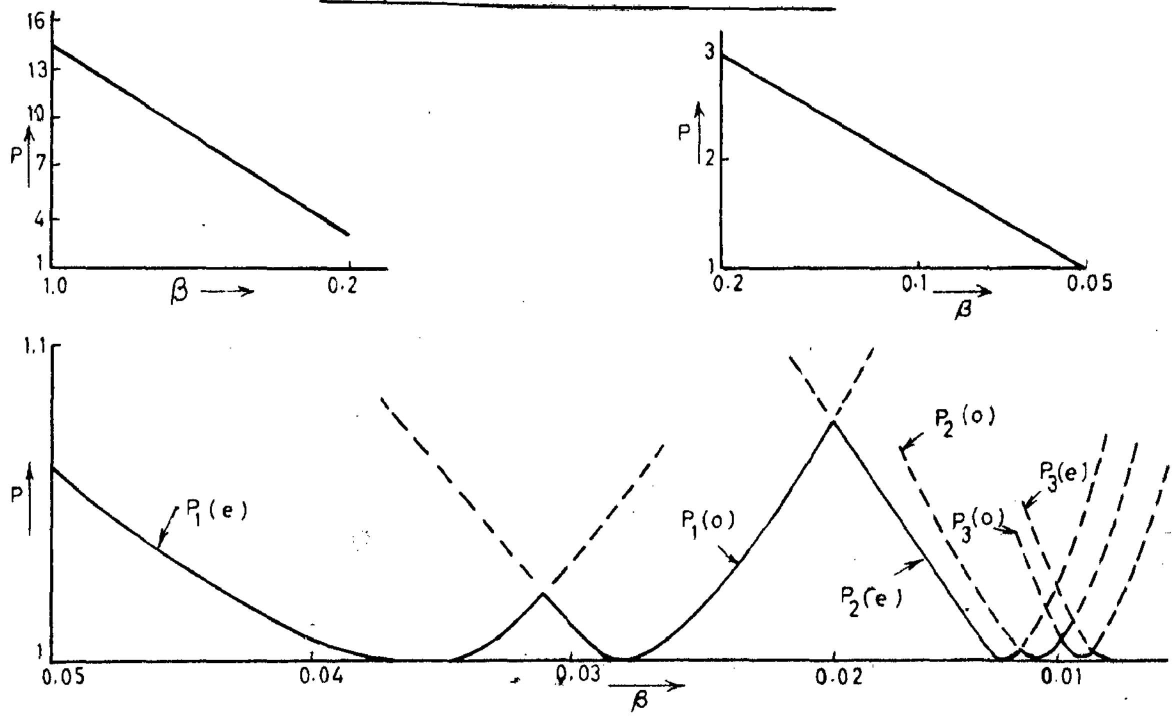

FIGURE-1

To actually find the critical load for any given shell in plan we determine β and then from the figure find critical value of p. Using the formula,

$$p_{cr} = \frac{4E\beta^2 P}{\sqrt{12(1-\nu^2)}} \cdot \frac{h^4}{b^4},$$

the critical load can easily be obtained.

The critical curve in the figure has been shown only for values of β as small as 0.01. It seems likely that for values of β smaller than this, the critical curve will remain very close to the minimum line at 1 for the value of P.

Hence for $\beta < 0.01$ i.e. $h > 100\,t$

$$P_{cr} = \frac{4E}{\sqrt{12(1-\nu^2)}} \cdot \frac{h^2 t^2}{b^4}$$

The results obtained here may be extended to hyperbolic paraboloidal shells where $a \neq b$. But for each value of α i.e. $\frac{a}{b}$, a complete new calculation from the original equation would have to be made and a new curve analogous to this would have to be plotted.

<u>Comment.</u>

The curves do not seem to be significant in generalising the result, because there is no regular variation. The spaces between the triangular portions (e.g. $P_1^{(o)}$, $P_2^{(e)}$, 1) are also not varying in a regular fashion. Moreover the contention of the author that the curve will be quite close to P=1 line after $\beta < 0.01$, does not seem to be final, unless actually the curves are extended taking more terms in the series expansion. This shows also that the buckling load is not a simple characteristic of the ratio $\frac{t}{h}$, probably the ratio $\frac{h}{a}$ or $\frac{h}{b}$ may be also significant or even more important than the ratio $\frac{t}{h}$. Hence curves with ratios of different parameters as abscissae have to be plotted until a regular relationship can be evolved which can be further verified by actual tests. As suggested by some investigators the buckling strength may be mainly a function of the shell rise 'h' (if not soley so) as compared to the span length 'a', the shallow shells buckling at much lower loads.

However, the limit of shallowness or flatness for buckling considerations has to be differentiated from the limit for validity of membrane analysis, as the few authors have shown that upto the rise to span ratio of about one fifth or one sixth the second order terms can be safely neglected and membrane theory applied. According to A.L. Parme(11) " One question that arises about these shells is the degree of flatness that can be used without invalidating the membrane analysis. This depends to a large extent on the magnitude of the secondary bending moments caused by axial strain. The analysis presented is based on a satisfaction solely of the equilibrium of forces and no attention is given to the compatability between strains and stresses. For the usual rise of $\frac{h}{a} = \frac{1}{5}$ or $\frac{h}{b} = \frac{1}{5}$, the effect of axial strains is unimportant and can be ignored safely. However, when the ratio $\frac{h}{a}$ decreases, the effect of axial strains begins to exert a dominant influence on the behaviour of the shell."

However, it can be pointed out that Reissner's formula is exactly the same as that obtained by Ralston for the range of $\beta < 6.01$ i.e. the rise is more than one hundred times the thickness of the shell. Thus the Reissner's formula is a special case of Ralston's results for $h > 100\ t$.

__Energy Method.__

A shallow hyperbolic paraboloid of side 'a' and rise 'h' is considered having equation as $z = \frac{h}{a^2} \cdot xy$.

The coordinates being as shown (Figure No.2)

GEOMETRY OF H.P. SHELL

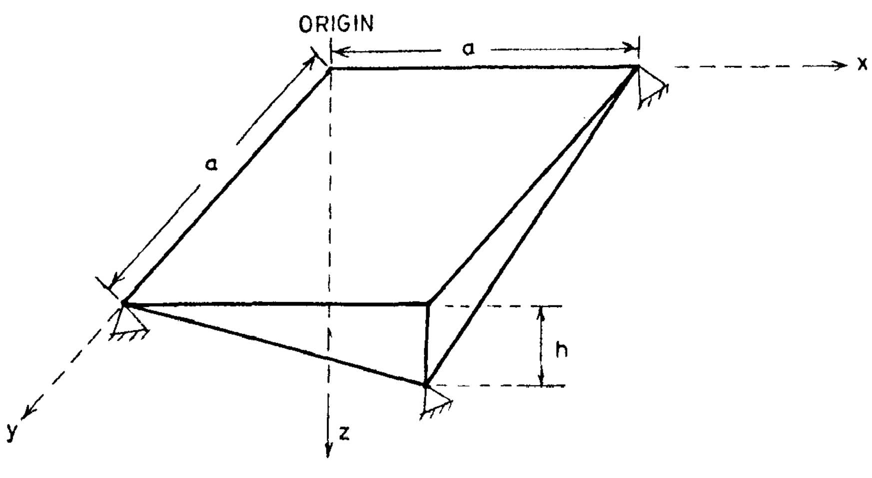

FIGURE-2

The shell is assumed to be framed between edge members which are simply supported at their corners. Membrane analysis results in

$$N_x = N_y = 0$$

$$N_{xy} = -q \cdot \frac{a^2}{2h}$$

The shear stress N_{xy} is transmitted to the supporting members at the shell edges.

Disregarding the conditions of compatability between shell and edge member and assuming that the uniformly distributed shear forces follow the deformed axis of the member, an elementary buckling analysis for this supporting member results in a critical load equal to (19)

$$\left[N_{xy}\right]_{cr} = 18.95 \frac{EI}{a^3} \quad .$$

Since additional strength is supplied to the edge member by the attached shell, it must be concluded that this buckling load constitutes <u>a possibly extremely conservative lower bound.</u>

The authors(17) have made use of Ritz minimising method of the potential energy of the system. The total strain energy consists of two parts:

1. Strain Energy V_1 of a plate subjected to direct and bending stresses (neglecting stretching of the middle surface) is equal to (20).

$$V_1 = \frac{1}{2}\iint\left[N_x\left(\frac{\partial w}{\partial x}\right)^2 + N_y\left(\frac{\partial w}{\partial y}\right)^2 + 2N_{xy}\frac{\partial w}{\partial x}\cdot\frac{\partial w}{\partial y}\right]$$

$$+ \frac{1}{2}\iint D(x,y)\left[\left(\frac{\partial^2 w}{\partial x^2} + \frac{\partial^2 w}{\partial y^2}\right) - 2(1-\nu)\right.$$

$$\left.\left\{\frac{\partial^2 w}{\partial x^2}\cdot\frac{\partial^2 w}{\partial y^2} - \left(\frac{\partial^2 w}{\partial x dy}\right)^2\right\}\right]dA$$

where $D(x,y)$ is the flexural stiffness of the structure at(x,y) and is the Poisson's ratio.

2. The strain energy V_2 corresponding to the stretching of the mid-surface of the shell is equal to (3).

$$V_2 = \frac{Et}{2(1-\nu^2)}\iint\left[(\epsilon_{\bar{x}} + \epsilon_{\bar{y}})^2 - 2\ (1-\nu)(\epsilon_{\bar{x}}.\epsilon_{\bar{y}} - \frac{1}{4}\epsilon_{\bar{xy}})\right] dA$$

where $\epsilon_{\bar{x}}$, $\epsilon_{\bar{y}}$ are the strains due to stretching of the middle surface of the shell.

To relate the middle surface strains to the displacements we express the in plane displacements U_x, U_y of the shell in terms of those of the middle surface displacements $\bar{U}_x$, $\bar{U}_y$,

$$U_x = \bar{U}_x - w\frac{\partial z}{\partial x},\quad U_y = \bar{U}_y - w\frac{\partial z}{\partial y}$$

and then differentiate to obtain the strains. Now since z and w are small for shallow shells under small deflections, the higher order terms in these variables can be dropped. Thus we obtain

$$\epsilon_x = \frac{\partial \bar{U}_x}{\partial x} \; ; \; \epsilon_y = \frac{\partial \bar{U}_y}{\partial y}$$

$$\epsilon_{xy} = \frac{\partial \bar{U}_x}{\partial x} + \frac{\partial \bar{U}_y}{\partial y} = \frac{2h}{a^2} \cdot w.$$

Neglecting the middle surface displacements $\bar{U}_x$ and $\bar{V}_y$ as assumed by Bleich and Salvadori (21) we get

$$\epsilon_x = 0, \; \epsilon_y = 0, \; \epsilon_{xy} = -\frac{2h}{a^2} \cdot w$$

Hence, $$V_2 = \frac{Eh^2 t}{a^4} \iint w^2 dA.$$

Thus the total internal strain energy of the structure is given by the expression

$$V = \frac{1}{2} \iint \left[N_x \left(\frac{\partial w}{\partial x} \right)^2 + 2N_{xy} \frac{\partial w}{\partial x} \cdot \frac{\partial w}{\partial y} + N_y \left(\frac{\partial w}{\partial y} \right)^2 \right] dA$$

$$+ \frac{1}{2} \iint D(x,y) \left[\left(\frac{\partial^2 w}{\partial x^2} \right)^2 + 2 \left(\frac{\partial^2 w}{\partial x \partial y} \right)^2 + \left(\frac{\partial^2 w}{\partial y^2} \right)^2 \right] dA$$

$$+ \frac{Eh^2 t}{a^4} \iint w^2 dA$$

The strain energy as given above is exactly the strain energy of a plate on an elastic foundation with the foundation modulus $\frac{2Eh^2t}{a^4}$. Hence, the problem reduces to that of a plate on elastic foundation, as already observed by Bleich and Salvadori (21).

The potential energy has been evaluated in four parts for the entire structure:-

1. The shell alone for which

$$N_x = N_y = 0, \quad N_{xy} = -\frac{qa^2}{2h}$$

and $D_{(xy)} = D$

2. The edge beams parallel to x-axis, for which

$$N_y = N_{xy} = 0, \; N_x = -\frac{qa^2}{2ta_1}.x$$

and $D(x,y) = \frac{EI_a}{a_1}$

where a_1 is the width and EI_a is the flexural rigidity of these beams.

3. The edge beams parallel to y-axis, for which,

$$N_x = N_{xy} = 0, \; N_y = -\frac{qa^2}{2tb_1}.y$$

and $D(xy) = \frac{EI_b}{b_1}$, where b_1 is the width and EI_b the flexural rigidity.

4. Loss of potential energy due to the drop of the applied surface load q, through a distance w is

$$U = \int_0^a \int_0^b q \; w dx \; dy.$$

The expression for the total energy is thus obtained as

$$V - U = \frac{D}{2} \int_0^a \int_0^b \left[\left(\frac{\partial^2 w}{\partial x^2} \right)^2 + 2 \left(\frac{\partial^2 w}{\partial x \partial y} \right)^2 + \left(\frac{\partial^2 w}{\partial y^2} \right)^2 \right] dx dy$$

$$+ EI_a \int_0^a \left(\frac{\partial^2 w}{\partial x^2} \right)^2_{y=0} dx + EI_b \int_0^b \left(\frac{\partial^2 w}{\partial y^2} \right)^2_{x=0} dy$$

$$- k \left[\int_0^a \int_0^b \frac{\partial w}{\partial x} \times \frac{\partial w}{\partial y} \times d x \, dy + \int_0^a x \left(\frac{\partial w}{\partial x} \right)^2_{y=0} dx \right.$$

$$\left. + \int_0^b y \left(\frac{\partial w}{\partial y} \right)^2_{x=0} dy \right] + E_1 \int_0^a \int_0^b w^2 \, dx \, dy$$

$$- q \int_0^a \int_0^b w dx \; dy \qquad \text{where } k = q \frac{ab}{2h}$$

$$\text{and } E_1 = \frac{Eh^2 t}{a^2 b^2}$$

Buckling of Shell Including Edge Beams.

The case of buckling of the shell along with its four simply supported edge beams is considered, the boundary conditions being

$$w = 0 \text{ at } (x=0, a) \text{ and } (y=0, b)$$

$$M_x = 0 \text{ at } (x=0, a) \text{ and } M_y = 0 \text{ at } (y=0, b).$$

Satisfying these boundary conditions, the deformation may be assumed as,

$$w = \sum_{m=1}^{\infty} \sum_{n=1}^{\infty} A_{mn} \sin \frac{m\pi x}{a} \sin \frac{n\pi y}{b}$$

$$+ \sum_{m=1}^{\infty} B_m \sin \frac{m\pi x}{a} + \sum_{n=1}^{\infty} C_n \sin \frac{n\pi y}{b}$$

Substituting these deformations into the energy expression and minimising with respect to the coefficients A_{mn}, B_m, C_n, three simultaneous equations are obtained. The critical load can be obtained by equating the determinant of these coefficients to be equal to zero.

Considering $I_a = I_b = I$ and $m = n$, for the square shell and neglecting the term $\frac{1}{n^2}$ as compared to unity the critical load associated with the n^{th} buckling mode is obtained as

$$q_{n_{cr}} = \frac{\pi^2}{6} \cdot E. \left(\frac{h}{a}\right) \cdot n^2 \left[\left(\frac{t}{a}\right)^3 + \frac{24I}{a^4} \right]$$

$$+ \frac{4E}{\pi^2 n^2} \left(\frac{h}{a} \right)^3 \left(\frac{t}{a} \right)$$

To find the buckling mode for which the critical load takes its lowest value we can do this by trial and error for any particular shell. If, for convenience it is assumed that 'n' is continuous instead of having only integral values, we can set

$$\frac{\partial\, q n_{cr}}{\partial\, n} = 0$$

The error due to this simplification will be very small and on the safe side. We obtain

$$n_{cr}^2 = \frac{2}{\pi} \cdot \frac{h}{a} \cdot \sqrt{\frac{6}{\left(\frac{t}{a}\right)^2 + \frac{24I}{a^3 t}}}$$

and

$$q_{n_{cr}} = 2E \left(\frac{h}{a}\right)^2 \left(\frac{t}{a}\right)^2 \sqrt{\frac{2}{3}\left(1 + \frac{2EI}{Da}\right)}$$

BUCKLING CURVES

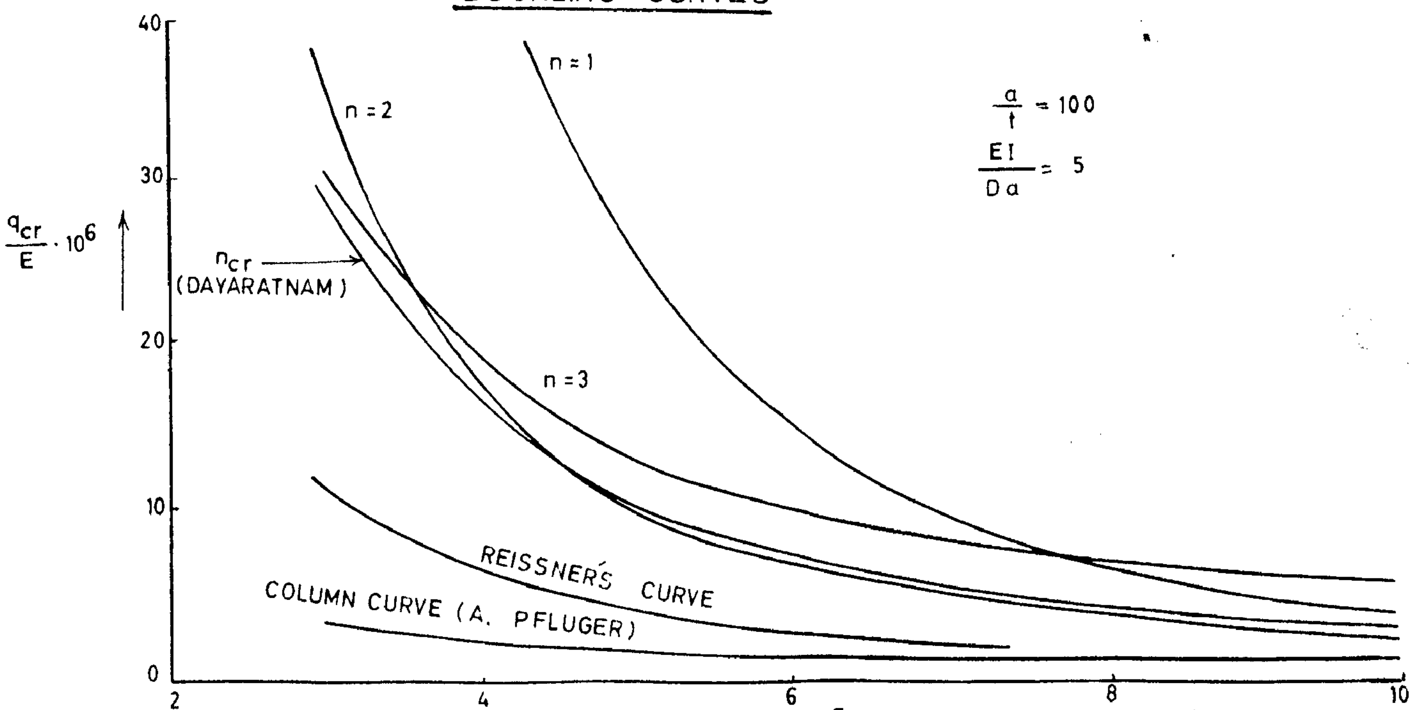

FIGURE-3

Results.

The values have been plotted (Figure No.3) for a square shell with $\frac{q_{cr}}{E}$ as ordinate against $\frac{a}{h}$ as abscissa for the various values of 'n' and it was found that the n_{cr} curve lies lower to other curves showing the accuracy of the minimizing procedure assuming variation of n as continuous.

Also it is seen that the buckling load of the beam without consideration of the shell interaction is considerably lower. A limiting condition of this would be that of the shell becoming infinitely thin so that the restraint offered by the shell to the edge beam should vanish. Simulating this condition by setting h = 0 and n=1 in the 1st expression for qn_{cr} we get $(N_{xy})_{cr} = 19.76 \frac{EI}{a^3}$ against $(N_{xy})_{cr} = 18.95 \frac{EI}{a^3}$ as obtained by A.P.Flueger, a close upper bound to the latter exact solution.

Reissner(7) had considered the possibility of <u>buckling of the shell without those of edge beams i.e.</u> the latter had sufficiently large flexural rigidity. On this basis q_{cr} is obtained equal to

$$\frac{2}{\sqrt{3}} E \left(\frac{h}{a}\right)^2 \left(\frac{t}{a}\right)^2 ,$$

and this curve is also plotted for comparison, which lies lower to the critical curve qn_{cr} however higher to the pure column curve of A.P. Pflueger.

The authors attempted to compare these two buckling modes i.e. one considering buckling of shell with edge beams and second that of shell only and they found that for all positive value of $\frac{EI}{Da}$ the second case controlled in the examples considered by them. It could be concluded, therefore, that for all cases, wrinkling of the shell will occur prior to buckling of the edge beams according to small deflection theory. However considering the figure No.4 which indicates the shape of the load-deflection curve,

LOAD DEFLECTION CURVE FOR H.P. SHELL

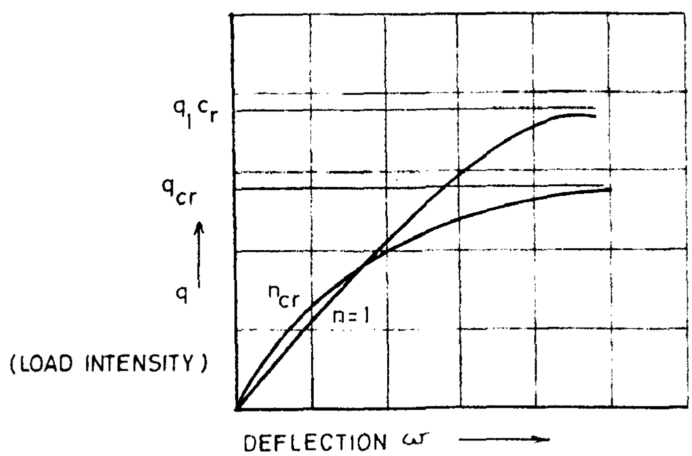

FIGURE-4

we observe that considerable deflections of non-linear ~~deflections of non-linear~~ nature may be expected prior to the occurrence of buckling and may be of importance.

CHAPTER III

DESIGN OF THE SHELL

3.1 Design Dimensions.

112 FT x 112 FT c/c in plan.

Rise of the corners (diagonally opposite)

= 20 ft and 58.3 ft respectively with respect to the other two which are at same level.

Design Load = 70p.s.f.

SHELL DIMENSIONS

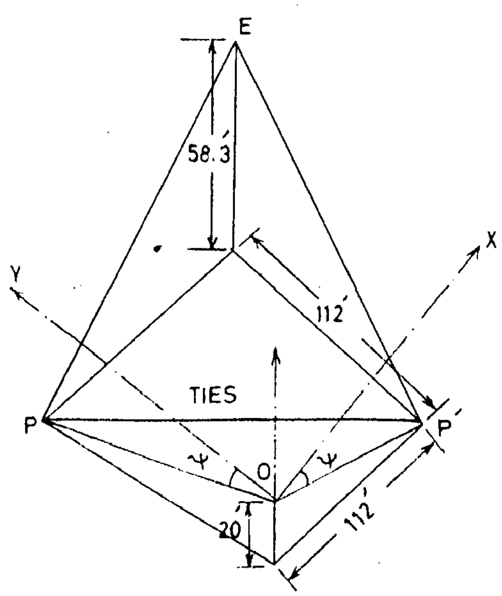

FIGURE_5

Let the hyperbolic paraboloid be OP' EP such that points P and P' are at the same level and 20 ft. lower to O and E is 58.3 ft. higher to P and P'.

If the points O, P and P' were at the same level with the rise of E being 'h', then taking x, y and z axes as shown with origin at O, the equation to the hyperbolic paraboloid would have been $z = \frac{h}{a^2} xy$, where 'a' is the side of hyperbolic paraboloid in plan.

If the inclination of OP and OP' with lines OX and OY respectively be ψ in the vertical planes, the equation to the hyperbolic paraboloid can be expressed as

$$z = \frac{h}{a^2} xy - (x+y) \tan\psi$$

where $\tan\psi = \frac{20}{112}$

To calculate the value of h, we substitute the coordinates of point 'E' in above.

$$38.3 = \frac{h}{112^2} \times 112 \times 112 - 2 \times 112 \times \frac{20}{112}$$

$$\text{or} \quad h = 38.3 + 40 = 78.3$$

$$\therefore \quad z = 0.00624xy - 0.1786\,(x+y)$$

Table No.1

Height of the shell points above the ground level

(z=0,00624 xy - 0,1786(x+y)   ,Ht. 48+z

x \ y	0	8	16	24	32	40	48
0	48,000	46.571	45,142	43,713	42,284	40,855	39,425
8	46,571	45,542	44,512	43,482	42,452	41,422	40,393
16	45,142	44,512	43,882	43,252	42,622	41,492	41,362
24	43,713	43.482	43,252	43,020	42,789	42,559	42,328
32	42,284	42,452	42,622	42,789	42,959	43,128	43,297
40	40,855	41,422	41,992	42,559	43,128	43,695	44,264
48	39,425	40,393	41,362	42,328	43,297	44,264	45,233
56	38,000	39,368	40,733	42,098	43.465	44,831	46,198
64	36,580	38,343	40,103	41,866	43,632	45,395	47,162
72	35,150	37,313	39,476	41,638	43,808	45,976	48,139
80	33,710	36,281	38,841	41.402	43,968	46,528	49,092
88	32,290	35,261	38,214	41.176	44,194	47,108	50,073
96	30,860	34,221	37,582	40,942	44,311	47,671	51.041
104	29,430	33,182	36,946	40,702	44,476	48,232	52,008
112	28,000	32,160	36,320	40,480	44,640	48,800	52,960

Continued...

NB. To avoid minus signs the height of the point O has been assumed as 48 ft. above the ground level arbitrarily.

x \ y	56	64	72	80	88	96	104	112
0	38.000	36.580	35.150	33.710	32.290	30.860	29.430	28.000
8	39.368	38.343	37.313	36.281	35.261	34.221	33.182	32.160
16	40.733	40.103	39.476	38.841	38.214	37.582	36.946	36.320
24	42.098	41.866	41.638	41.402	41.176	40.942	40.702	40.480
32	43.465	43.632	43.808	43.968	44.144	44.311	44.476	44.640
40	44.831	45.395	45.966	46.528	47.108	47.671	48.232	48.800
48	46.198	47.162	48.139	49.092	50.073	51.041	52.008	52.960
56	47.562	48.924	50.300	51.650	53.027	54.392	55.756	57.120
64	48.924	50.294	52.447	54.210	55.980	57.736	59.480	61.210
72	50.300	52.447	54.635	56.780	58.960	61.130	63.240	65.440
80	51.650	54.210	56.780	59.780	61.900	64.440	67.000	69.600
88	53.027	55.980	58.960	61.900	64.880	67.848	70.760	73.760
96	54.392	57.736	61.130	64.440	67.848	71.200	74.520	77.920
104	55.756	59.480	63.240	67.000	70.760	74.520	78.280	82.040
112	57.120	61.210	65.440	69.600	73.760	77.920	82.080	86.300

Concluded......

3.2 Membrane Analysis and Design.

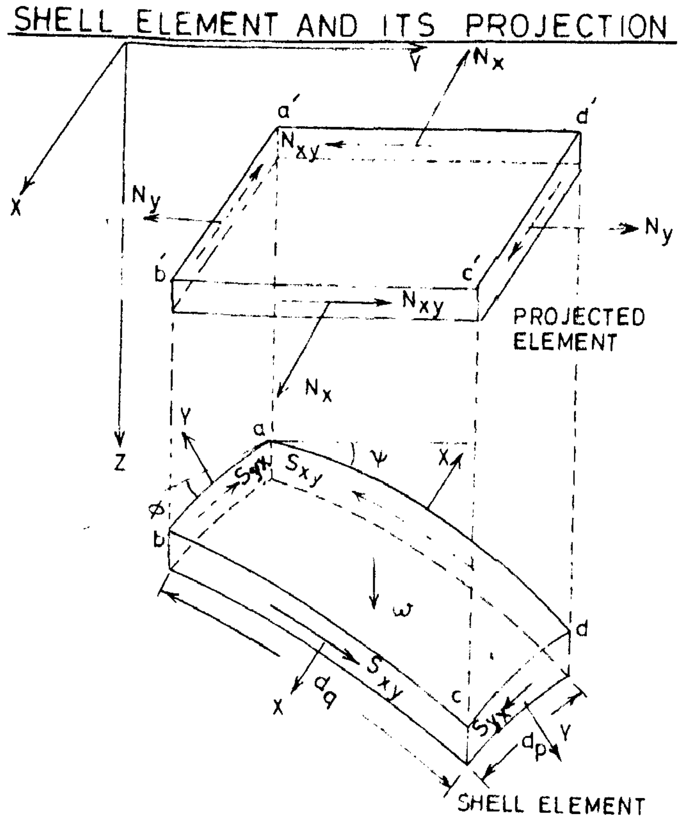

FIGURE 6

Forces acting on Shell-Element.

S_x and S_y are direct forces for unit length, and S_{xy} is the shearing force also per unit length. N_x, N_y and N_{xy} are forces per unit length acting on the projected element. dp and dq are the lengths of shell-element along x and y axes.

The tensile forces are taken positive and shears creating tension along positive direction of the diagonal are taken positive. The surface load 'W' is considered positive when acting downwards.

The forces acting on the element are reduced into components that are parallel to the coordinate system but have their direction tangential to the surface. Hence, force δy is parallel to zy plane but is inclined at an angle 'ψ' to the xy plane.

The expressions for the equilibrium of forces parallel to the various axes are considerably simplified if the actual forces are transformed into fictitious forces acting on the projected area of the element;

The analytical details and the resolution of forces in three directions along with the simplifying assumptions need not be given here, as they can be available in the reference (23). The results, however, are as follows:-

$$N_x = S_x \sqrt{\frac{1 + q^2}{1 + p^2}}$$

$$N_y = S_y \sqrt{\frac{1 + p^2}{1 + q^2}}$$

i.e. $$S_x = N_x \sqrt{\frac{1 + p^2}{1 + q^2}} \quad \text{and} \quad S_y = N_y \sqrt{\frac{1 + q^2}{1 + p^2}}$$

$$S_{xy} = N_{xy}$$

$$p = \frac{dz}{dx} = 0.00624y - 0.1786$$

$$q = \frac{dz}{dy} = 0.00624x - 0.1786$$

$$r = \frac{d^2z}{dx^2} = 0$$

$$s = \frac{d^2z}{dx\,dy} = 0.00624$$

$$t = \frac{d^2z}{dy^2} = 0$$

$$p_v = po\sqrt{1+p^2+q^2} \approx po\left(1 + \frac{p^2}{2} + \frac{q^2}{2}\right)$$

where po and p_v are the loads per square foot of the surface and horizontal projection respectively.

Equations of Equilibrium

In z-Direction

$$N_x \frac{d^2z}{dx^2} + 2N_{xy}\frac{d^2z}{d_x\,d_y} + N_y\frac{d^2z}{dy^2} + z = 0;$$

$$z = -p_v$$

$$\therefore\ 2N_{xy}.S = p_v = po\left(1 + \frac{p^2}{2} + \frac{q^2}{2}\right)$$

$$2\times 0.00624\, N_{xy} = p_o \cdot \Big[1 + \tfrac{1}{2}(0.00624y - 0.1786)^2 + \tfrac{1}{2}(0.00624x - 0.1786)^2 \Big]$$

$$N_{xy} = 80\, p_o \cdot \Big[1 + \tfrac{1}{2}\,(0.00624y - 0.1786)^2 + \tfrac{1}{2}\,(0.00624x - 0.1786)^2 \Big]$$

In x-direction,

$$\frac{d\,N_x}{d_x} + \frac{d\,N_{xy}}{d_y} + X = 0\,, \quad X = 0$$

$$\therefore \int d\,N_x = - \int - \frac{d\,N_{xy}}{d_y}\, dx$$

$$= - \frac{p_o}{2} \int (0.00624y - 0.1786)\,d_x + f\,(y)$$

OR, $$N_x = - \frac{p_o}{2}\, x\,(0.00624y - 0.1786) + f(y)$$

In y-direction, we get similarly

$$N_y = \int dN_y$$

$$= - \frac{p_o}{2} \cdot y\,(0.00624x - 0.1786) + f(x)$$

Boundary Condit.

At the edge $x = 0, N_x = 0$

and at $y = 0, N_y = 0$

Substituting these we get,

$$f(x) = f(y) = 0$$

and

$$N_x = -po \frac{x}{2} (0.00624y - 0.1786)$$

$$N_y = -po \frac{y}{2} (0.00624x - 0.1786)$$

Now $S_{xy} = N_{xy}$

$$S_x = N_x \sqrt{\frac{1 + p^2}{1 + q^2}}$$

and $S_y = N_y \sqrt{\frac{1+q^2}{1+p^2}}$

The forces N_x, N_y, $N_{xy} = S_{xy}$, S_x, and S_y are calculated and given in the accompanying table (Table No.2).

Table No.2

x	y	$N_x = p_o x$	$N_y = p_o x$	$N_{xy} = S_{xy} = p_o x$	p	q	$\sqrt{\frac{1+p^2}{1+q^2}}$	$S_x = p_o x$	$S_y = p_o x$
112	0	10.000	0	92.2	-0.1786	0.5194	0.903	9.03	0
	16.0	4.410	-4.15	93.3	-0.0788	0.5194	0.915	4.03	-4.54
	32.0	- 1.174	-8.31	90.9	+0.0210	0.5194	0.890	- 1.04	-9.33
	48.0	- 6.760	-12.45	91.6	+0.1208	0.5194	0.894	- 6.04	-13.94
	64.0	-12.370	-16.61	92.7	0.2206	0.5194	0.909	-11.29	-18.29
	80.0	-17.950	-20.75	94.9	0.3204	0.5194	0.933	-16.75	-22.23
	96.0	-23.500	-24.90	97.8	0.4202	0.5194	0.963	-22.65	-25.85
	112.0	-29.100	-29.10	101.5	0.5200	0.5194	1.000	-29.10	-29.10

Maximum Tension or Compression is given by

$$S_m = \frac{S_x + S_y}{2} \pm \sqrt{\left(\frac{S_x - S_y}{2}\right)^2 + S_{xy}^2} \text{ , if we}$$

neglect the effect of obliquity angle.

At (112', 112'), $S_x = S_y = -29.10\ p_o$ and $S_{xy} = 101.5\ p_o$

$\therefore$ Maximum tension $= (-29.10 + 101.5)p_o$ $= 82.4\ p_o$

$= 5768$ lbs/ft.

Maximum compression $= (-29.10 - 101.57)p_o$

$= 130.6\ p_o$ $= 9142$ lbs/ft.

At point (0,112) the value of S_{xy} will be same as at (112,0) and $S_x = 0$, $S_y = 9.03\ p_o$

$\therefore S_{xy} = 92.2\ p_o$

$\therefore$ Maximum forces $= 4.525\ p_o \pm p_o \sqrt{20.3 + 8490}$

$= (4.5 \pm 92.4)p_o$

$\therefore$ Maximum tension $= 96.9\ p_o = 6783$ lbs/ft.

Maximum compression $= 87.9\ p_o = 6153$ lbs./ft.

Checking Stresses.

4 ins. shell thickness is adopted $1:1\frac{1}{2}:3$ mix being used. Reinforcement = $\frac{1}{2}$ in. ∅ bars 5 ins. o/c in both directions along ruling lines at the mid-depth of the slab.

∴ Effective area in any direction. $= \frac{12}{5} \times 0.196 = 0.47$ sq.in./ft.

Maximum compressive stress in concrete. $= \frac{9142}{12x4 + 0.47x13}$

$= 169$ p.s.i.(safe)

Maximum tensile stress in steel. $= \frac{6783}{0.47}$

$= 14440$ p.s.i. (safe),

Assuming all tension is taken by steel.

Maximum composite tension. $= \frac{6783}{12x4+0.47x13} = 125.4$ p.s.i.

There will be no cracks, the ultimate tensile strength of concrete being about 280 p.s.i.

3.3 Bending Analysis (Vreedenburgh's Method) and Design.

Shell panel is assumed clamped at the edges.

Characteristic length $= \frac{0.76\sqrt{t}}{\sqrt[4]{k_1^2 + k_2^2}}$

where t = shell thickness

and k_1, k_2 are the principal curvatures of the shell at edge point.

Negative clamping moment = $M_o = -\frac{1}{2} p_o \lambda^2$ per unit width

Shear force = $q_o = p_o \lambda$

Shell moment (positive) = $m_1 = +0.10\ p_o \lambda^2$ at 1.57 from the edge.

Calculation of characteristic length.

$$\text{Curvature} = \frac{\frac{d^2z}{dx^2}}{\left[1 + \left(\frac{dz}{dx}\right)^2\right]^{3/2}}$$

Equation to the shell is, $z = 0.00624xy - 0.1786(x+y)$

Rotating the axes by 45°, the equation becomes

$$z' = 0.00312\ (x'^2 - y'^2) - 0.252x' \quad \text{(Figure No.7)}$$

ROTATION OF AXES

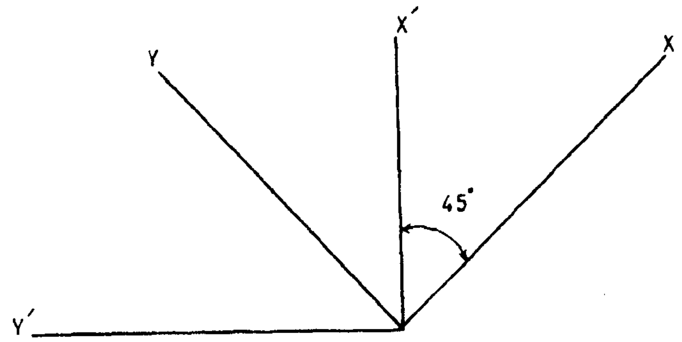

FIGURE-7

This is done since along the new axes twist term $\frac{\partial^2 z'}{\partial x' \partial y'}$ is zero and curvatures along these are the principal curvatures.

$$\frac{dz'}{dx'} = 0.00624x' - 0.252$$

$$\frac{dz'}{dy'} = -0.00624\, y'$$

$$\therefore \frac{d^2 z'}{dx'^2} = -\frac{d^2 z'}{dy'^2} = 0.00624 \text{ and } \frac{d^2 z'}{dx'\, dy'} = 0$$

$$\therefore k_1 = \frac{0.00624}{\left\{1 + (0.00624x' - 0.252)^2\right\}^{3/2}}$$

And $$k_2 = \frac{-0.00624}{\left\{1 + (-0.00624\, y')^2\right\}^{3/2}}$$

For the point (0,112) in x-y system,

$$x' = y' = 79.2 \text{ ft.}$$

$$\therefore k_1 = \frac{0.00624}{\left\{1 + (0.494 - 0.252)^2\right\}^{3/2}} = 0.00573$$

$$k_2 = \frac{-0.00624}{(1.244)^{3/2}} = -0.0045$$

$$\therefore \quad \lambda = \frac{0.76\sqrt{0.375}}{0.001\sqrt{32.8+20.25}} = 6.38 \text{ ft.}$$

$$m_0 = -\frac{1}{2} \times 70 \times 6.38^2 = 1422 \text{ lbs.ft./ft.}$$

$$q_0 = 70 \times 6.38 = 446.2 \text{ lbs/ft.}$$

$$m_1 = 0.1 \times 70 \times 6.38^2 = 284.4 \text{ lbs.ft./ft.}$$ at 10 ft. from the edge.

Design for Moments

Thickness of the shell will be increased to 6 ins. in 14 ft. near the edge and then reduced to 4 ins. gradually. The reinforcement already provided i.e. $\frac{1}{2}$ in. dia. 5 ins.c/c will be bent to be kept at bottom at 14 ft. from edges with 1 in. cover to the centre of the lower bars. A mesh will be provided of the same size at the top as well in 10 ft. width all along the edges, thus, giving $\frac{1}{2}$ in. ∅ bars 5 ins. c/c in both directions at top and bottom.

Checking Stresses.

Compressive Stress in Concrete. (Figure No.8)

SHELL-SLAB SECTION AT THE EDGES

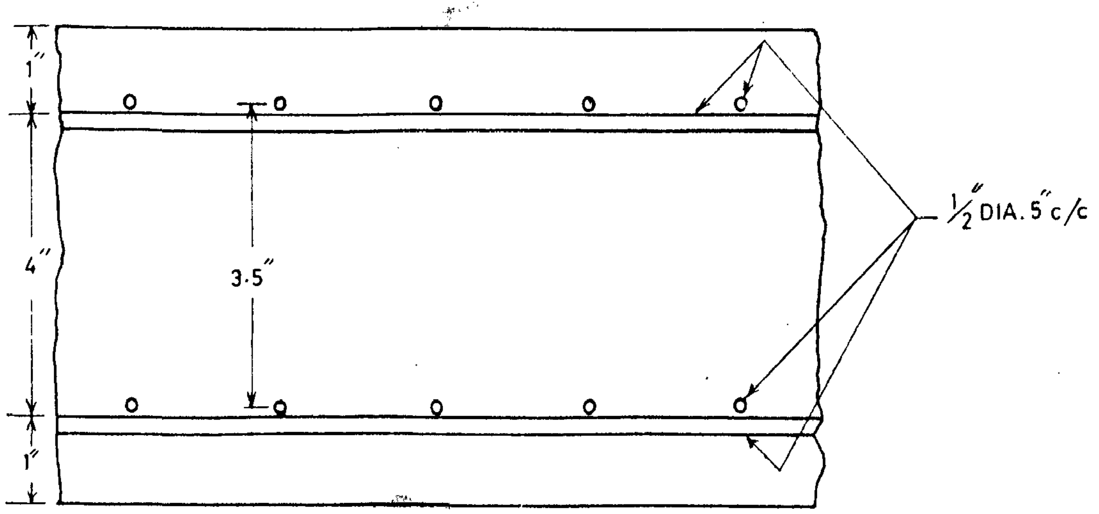

FIGURE_8

$P = 9142$ lbs. (direct force)

$M = 1422$ ft. lbs. (bending moment)

$A_c = A_t = \frac{12}{5} \times 0.196 = 0.47$ sq.in. in each direction.

$A = 12x6 + 2x0.47 \times 13$

$= 72 + 12.2 = 84.4 \; in^2$

$I \approx \frac{12x6^3}{12} + 2 \times 0.47 \times 1.75^2 \times 13$

$= 253.4 \; in^4$

$C \approx \frac{9142}{84.4} + \frac{1422 \times 12 \times 3.0}{253.4}$ (on safer side)

$= 310$ p.s.i. (safe)

Tensile Stress in Steel.

$M = -1422$ lbs.ft.

$P = 9142$ lbs.

$\therefore e = \frac{1422 \times 12}{9142}$

$= 1.87$ ins.

Assuming conservatively that all the concrete has cracked,

SLAB_SECTION AT THE EDGES

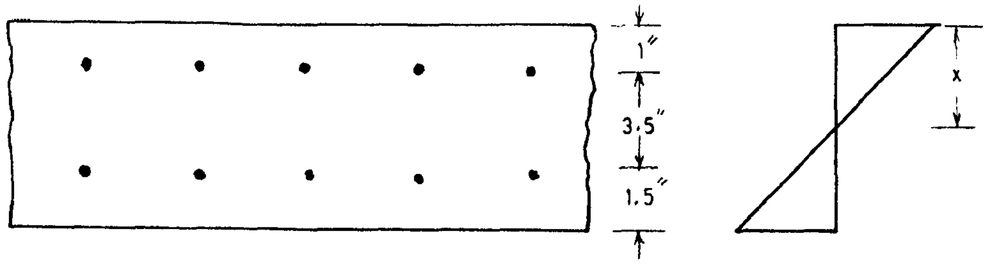

FIGURE_9

$0.47 \times 13(x-1.0) = 14 \times 0.47(4.5-x)$

$\therefore x = 2.82$ ins.

and 4.5 ins-2.82 ins.= 1.68 ins.

Taking moments about compression steel at bottom

$0.47 \times t \times 3.5 = 9142\ (1.87+1.68)$

$\therefore t = \dfrac{9142 \times 3.55}{0.47 \times 3.5} = 19760$ p.s.i

which is slightly higher than the permissible value of 18000 p.s.i. but since the formula for moments is empirical and changing the spacing of bars would be inconvenient as well as providing extra bars will become uneconomical;

the slight overstress, if at all is allowed and no extra reinforcement is provided.

3.4 Design of Edge Beams (Figure No.10)

DIRECTION OF AXIAL FORCES

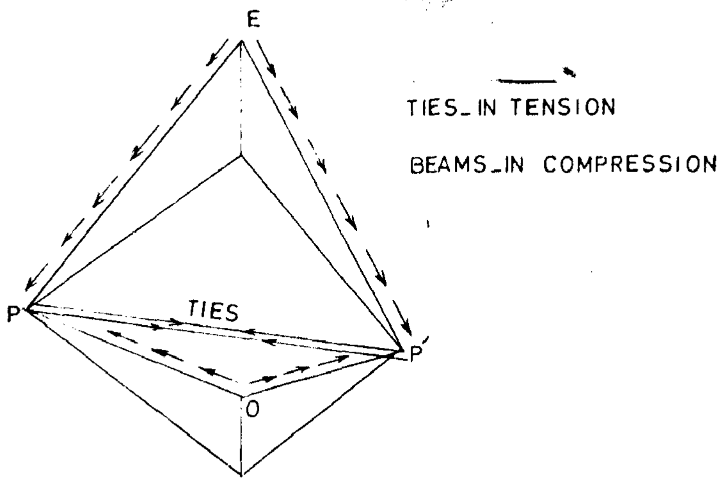

FIGURE_10

$$OP,\ OP' = \sqrt{112^2 + 20^2} = 114 \text{ ft.}$$

$$PE,\ PE' = \sqrt{112^2 + 58.3^2} = 126.5 \text{ ft.}$$

Edge beams will be simply supported at their corners. Ties will be provided along PP' to take up the tension. The compression builds up in beams from E and O towards P and P' respectively from minimum values at E and O, to maximum values at P and P'.

Beams OP and OP'

$$S_{xy} = 80.70 \left\{ 1 + \frac{1}{2} \cdot 0.1786^2 + \frac{1}{2} (0.00624x - 0.1786)^2 \right\} \text{lbs/ft.}$$

$$= 5780 + 0.1089x^2 - 6.24x$$

Total compressive force at P or P' in OP or OP' respectively,

$$= F_1 \text{ (say)} = \int_0^{112} (5780 - 6.24x + 0.1089x^2) dx$$

$$= 6.6 \times 10^5 \text{ lbs.}$$

Force at O = 5780 lbs/ft.

Beams PE and P'E

For P'E, x = 112 ft. and y varies from 0 to 112 ft.

$$S_{xy} = 5600 \left\{ 1 + \frac{1}{2} (0.00624y - 0.1786)^2 + \frac{1}{2}(0.00624 \times 112 - 0.1786)^2 \right.$$

$$= 0.1089x^2 - 6.24y + 6400.$$

Total compressive force at P or P' in EP or EP' respectively,

$$= F_2 \text{(say)} = -\int_0^{112} (6400 - 6.24y + 0.1089y^2) \, d_y$$

$$= 7.35 \times 10^5 \text{ lbs.}$$

Force at E i.e. (112, 112) = 101.5 x 70 = 7105 lbs/ft.

Force in Tie say 'T'

Horizontal component of $F_1 = 6.6 \times 10^5 \frac{112}{114} = 6.5 \times 10^5$ lbs.

Horizontal component of $F_2 = 7.35 \times 10^5 \times \frac{112}{126.5} = 6.58 \times 10^5$ lbs.

$\therefore T = (6.5 + 6.58) \times 10^5 \times \sqrt{2} = 1.85 \times 10^6$ lbs.

Compressive Force Component due to self-weight of beams may be added to this while designing the section.

<u>Compression on columns at P or P' say C.</u>

$$C = (6.6 \times \frac{20}{114} + 7.35 \times \frac{58.3}{126.5})\times 10^5 \text{ lbs.}$$

$$= 4.625 \times 10^5 \text{ lbs.}$$

Component of self-weight of beams may be added to this while designing the sections.

<u>Design of Beams EP and EP'</u> (Fig.No.11)

BEAMS EP AND EP'

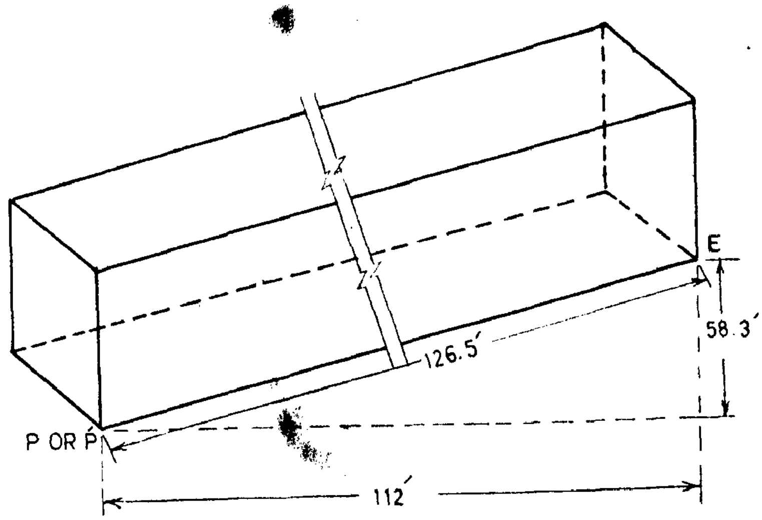

FIGURE_11

Section at Mid-span say Q Normal to Beam-axis.

39 ins.x115 ins. with 22 bars $1\frac{1}{2}$ ins. dia. at top and bottom both is provided.(Figure No.12)

BEAM-SECTION

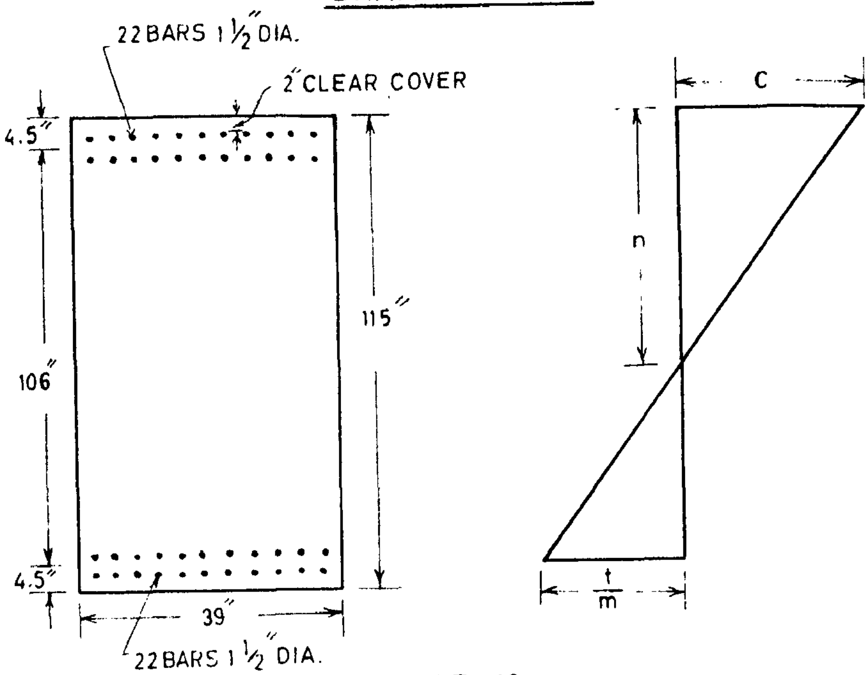

FIGURE_12

Self Load = 39x115 = 4485 lbs./ft.

It can be resolved into two components. The component perpendicular to beam axis can be considered to create bending moment as usual and the component parallel to beam axis will contribute towards the axial compression, which will be equal to $4485 \times \frac{58.3}{126.5}$ = 2067 lbs/ft. in magnitude, acting from E towards P.

$\therefore$ Total axial compression at P

$$= 7.35 \times 10^5 + 2067 \times 126.5$$
$$= 9.97 \times 10^5 \text{ lbs.}$$

Total axial compression at Q

$= 56\ \{(6400-3.12\times56+0.0363\times56^2)\}\ +(2067\times63.25)$

$= 4.86\times10^5$ lbs.

Component perpendicular to beam axis

$= 4485\times\frac{112}{126.5} \quad = 3980$ lbs./ft.

$\therefore M_Q \quad = \frac{3980\times126.5^2}{8}\times 12$ lbs.in.

$= 9.55\times10^7$ lbs.in.

$\therefore e \quad = \frac{9.55\times10^7}{4.86\times10^5} \quad = 196.5$ ins.

$\Sigma V \quad = 0$ gives

$$39\times n\times\frac{c}{2} + 22\times1.77\ t_o - 22\times1.77t \quad = 4.86\times10^5 \quad \ldots\ldots (i)$$

$$t_o \quad = \frac{n-4.5}{n}\times 13c \ (\text{since } m = \frac{40{,}000}{3F_c} = 14) \quad \ldots\ldots (ii)$$

$$t \quad = 14c\times\frac{110.5-n}{n} \quad \ldots\ldots (iii)$$

Taking moments about the tensile steel,

$$39\times n\times\frac{c}{2}\times(110.5-\frac{n}{3}) + 22\times1.77\times\frac{n-4.5}{n}\times13c\times106$$

$$= 4.86\times10^5\times(197+53)$$

Dividing (iv) by (i) after substituting

for t_o and t from (ii) and (iii)

$$\frac{19.5\times n\ (110.5-\frac{n}{3}) + 53600\times\frac{n-4.5}{n}}{19.5n + 505\times\frac{n-4.5}{n} - 544\times\frac{110.5-n}{n}} = 250 \quad \ldots\ldots (iv)$$

Or $2160n - 6.5n^2 + 53600 - \frac{241000}{n}$

$$= 4860n + 126300 - \frac{568000}{n} - \frac{15000000}{n} + 13600$$

Or, $6.5n^3 + 2720n^2 + 208700n - 15327000 = 0$

$\therefore$ n = 45 ins.

Equation (iv) gives

$$Cx\left\{19.5x95.5x45 + 53600x\frac{40.5}{45}\right\} = 250x4.86x10^5$$

or $C\left\{83900 + 48300\right\} = 250x4.86x10^5$

$\therefore$ $C = \frac{250x486000}{132200}$ = 918 p.s.i. (safe)

$\therefore$ $t = 14x918x\frac{65.5}{45}$ = 18700 p.s.i.

The extra bars prpvided for the tension will account for this slight increase in the value of the tensile stress in the steel than 18000 p.s.i.

End Reaction (normal) $= 39x115x\frac{112}{126.5}x\frac{126.5}{2}$

= 251,000lbs

Taking j = 0.86 (on the safer side)

Shear stress $= \frac{251000}{0.86x39x110.5}$ = 67.8 p.s.i.(safe)

Minimum number of bars required
for bond stress to be safe

i.e. 120 p.s.i. $= \frac{251000}{120x0.86x110.5x4.71}$ = 5.62

...ce bars provided are more than sufficient for bond.

For compression

0.8% of cross-sectional area $= \frac{0.8}{100} \times 39 \times 115$

$= 20.3$ bars $1\frac{1}{2}$ ins. dia.

Direct compressive stress at the end of beam without considering steel $= \frac{9.97 \times 10^5}{39 \times 115}$

$= 223$ p.s.i.

Hence resultant stress will be within safe limits even if only 22 bars i.e. 11 each at top and bottom are provided at the end upto 25 ft. as seen by testing the section there. However, the curtailment will be done at 22.5 ft. from the end as shown.

Two-legged stirrups $\frac{3}{4}$ ins. ϕ, 2 ft. c/c will be provided all along the length of the beam.

The beam must be provided for the torsion of 1422 lbs.ft./ft. coming at the edges from the slab, which has a negative moment of this value. It can safely be assumed to be uniform throughout the length of the beam.

Assuming the ends to be restrained for torsion by the beams in the perpendicular direction, the end torque

$$T = \frac{1422 \times 126.5}{2} \times 12 \text{ lbs.in} = 10.8 \times 10^5 \text{ lbs.in.}$$

Safe diagonal tension for 1:1.5:3 Reinforced Concrete =95 p.s.i.

Using H.J.Cowan's formula for torsion (24) and using hoops

$$T = 1.63A \frac{a_t \cdot t}{p} \text{ (taking } \lambda = 1.63)$$

A = area enclosed by reinforcement

= 33x100 (say)

= 3300 sq.ins.

Using $\frac{1}{2}$" dia. hoops,

a_t = 0.196 sq.in.

Shear stress would be maximum at the ends due to torsion.

$$S = \frac{T}{k\, b^2\, d} \text{ (for } \frac{d}{b} = \frac{115}{39} \text{ ; } k = 0.265)$$

$$= \frac{1422 \times 126.5 \times 6}{0.265 \times 39^2 \times 110} = 24.4 \text{ lbs/in}^2 \text{ (safe)}$$

Spacing of $\frac{3}{4}$ in. dia. hoops along length

$$= \frac{1.63 \times 3300 \times 0.442 \times 18000}{1422 \times 126.5 \times 6}$$

= 39.7 ins.

The two-legged stirrups already provided will suffice.

Length of hoops = $2\times(34+110)$ = 288 ins.

Total volume of hoops. $= \frac{126.5\times12}{24} \times 288 \times 0.442$

= 8050 cu.ins.

To provide equal volume longitudinally,

$$\text{required area} = \frac{8050}{126.5 \times 12}$$

$$= 5.3 \text{ in}^2$$

Area provided by four bars 1.5 ins. dia. is 7.08 in^2 Two bars on each side of the beam shall be provided in addition to the previous ones as shown in Figure No.13.

At ends other moments being zero, only the end torque shall be transferred from the neighbouring perpendicular beams as the negative bending moment whose magnitude is 10.8×10^5 lbs.in. while the curtailed section provided till end of beam with 11 bars each at top and bottom is able to take up much greater bending moment i.e. 8.0×10^7 lbs.in. and so no further provision of reinforcement is necessary.

BEAM REINFORCEMENT

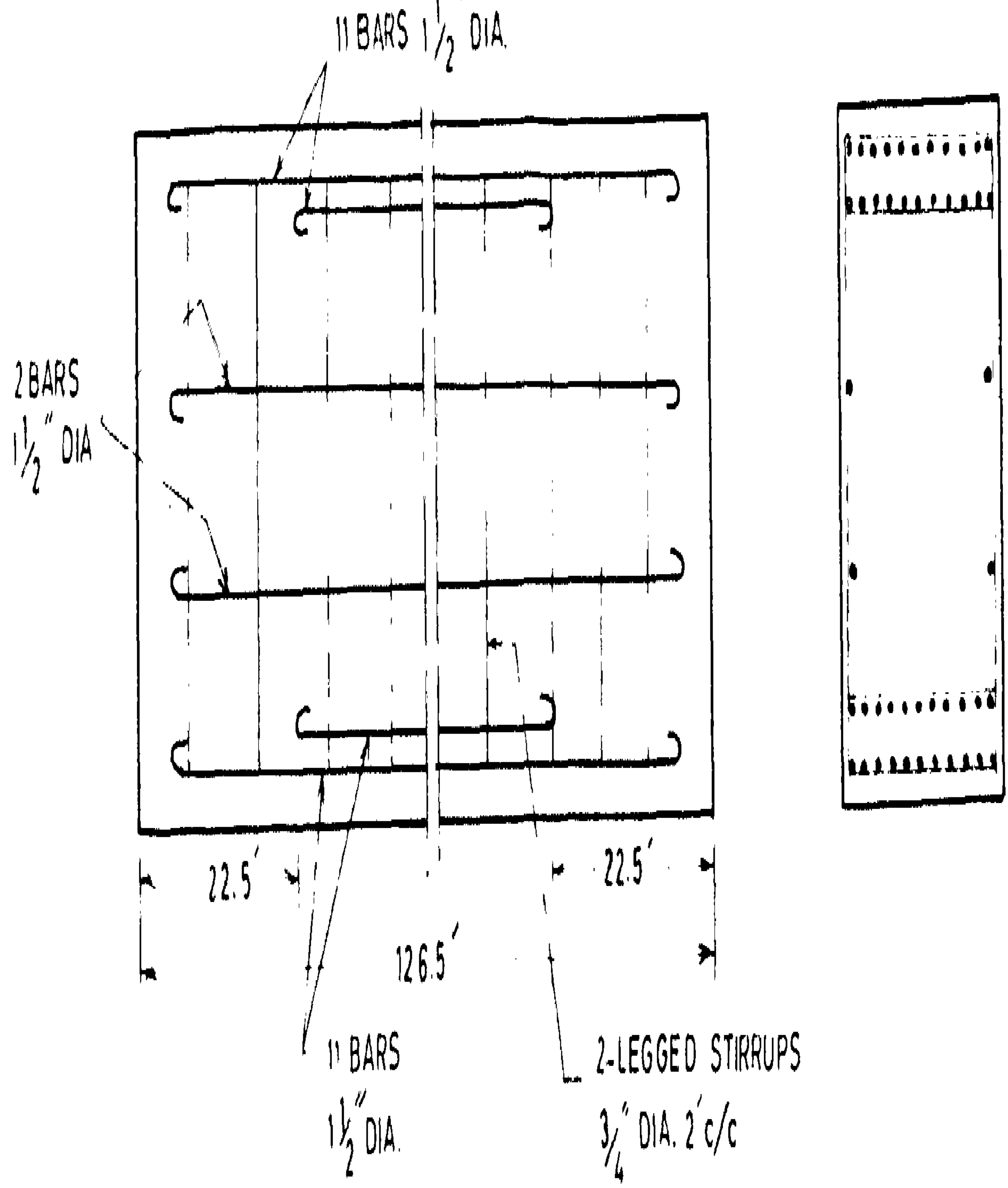

FIGURE_13

Beams OP and OP'

Same section will be provided, the curtailment being done at 19.5 ft. from the ends instead of 22.5 ft.

Design of Tie Bars.

$$\text{Tensile force} = 1.85\text{x}10^6 + \left\{39\text{x}115\text{x}\frac{58.3}{126.5}\text{x}126.5 + 39\text{x}115\text{x}\frac{20}{114}\text{x}114\right\} \Big/ \sqrt{2}$$

$$= 2.35\text{x}10^6 \text{ lbs.}$$

$$\text{Minimum steel area required} = \frac{2,35,0000}{18,000} = 131 \text{ sq.ins.}$$

For considerations of safety 200 sq.ins. may be provided.

3.5 Buckling loads according to different theories.

H.Schmidt's Formula

$$P_{cr} = 0.15 \frac{Et^2}{R_1\ R_2} = 0.15\ Et^2 .\ k_1 k_2$$

$$k_1 = \frac{0.00624}{\{1+(0.00624x'-0.252)^2\}^{3/2}}$$

$$k_2 = \frac{-0.00624}{\{1+(-0.00624y')^2\}^{3/2}} = \frac{-0.00624}{\{1+0.000039\ y'^2\}^{3/2}}$$

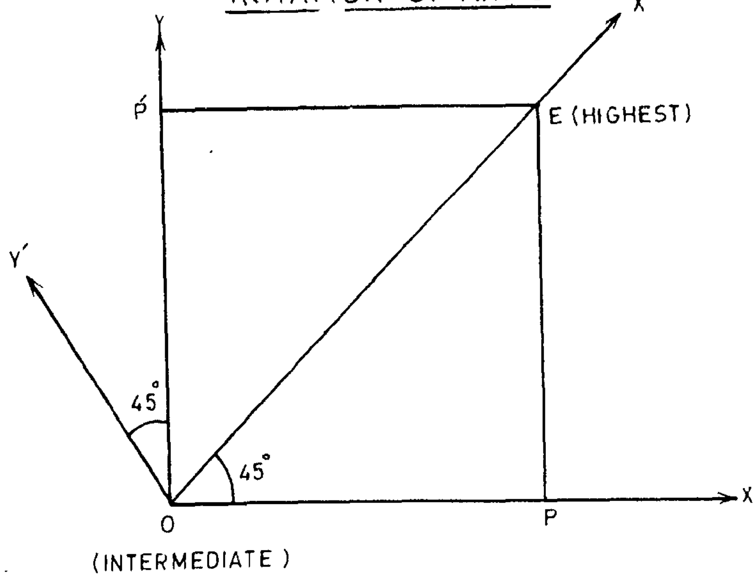

FIGURE-14

$$y' = \frac{y-x}{\sqrt{2}}$$

and $$x' = \frac{y+x}{\sqrt{2}}$$

<u>For the Point (112,112)</u>

$y' = 0 \; , \; x' = 112\sqrt{2}$

$\therefore \quad k_1 = \dfrac{0.00624}{\left\{1 + (0.988 - 0.252)^2\right\}^{3/2}}$

$= \dfrac{0.00624}{\left\{1 + 0.736^2\right\}^{3/2}}$

$= \dfrac{0.00624}{1.54 \times 1.24}$

$= 0.00327$

$k_2 = -0.00624$

$k_1 \, k_2 = -0.0000204$

<u>For the point (0,112)</u> <u>Same as for (112,0)</u>

$x' = y' = \dfrac{112}{\sqrt{2}} = 79.2$

$k_1 = 0.00573$ and $k_2 = -0.0045$

$\therefore \quad k_1 \, k_2 = -0.0000258$

<u>For the point (0,0)</u>

$x' = y' = 0$

$\therefore \quad k_1 = \dfrac{0.00624}{\left\{1+0.0634\right\}^{3/2}} = \dfrac{0.00624}{1.0634 \times 1.032} = 0.00569$

$k_2 = -0.00624$

$\therefore k_1k_2 = -0.0000355$

<u>For the point (56,56)</u> same as for (56,0)

$y' = 0, x' = 56\sqrt{2} = 79.2$

$$k_1 = \frac{0.00624}{\{1+(0.494-0.252)^2\}^{3/2}} = \frac{0.00624}{1.0585\times1.03}$$

$$= 0.00573$$

$k_2 = -0.00624 \quad , \quad k_1k_2 = -0.0000358$

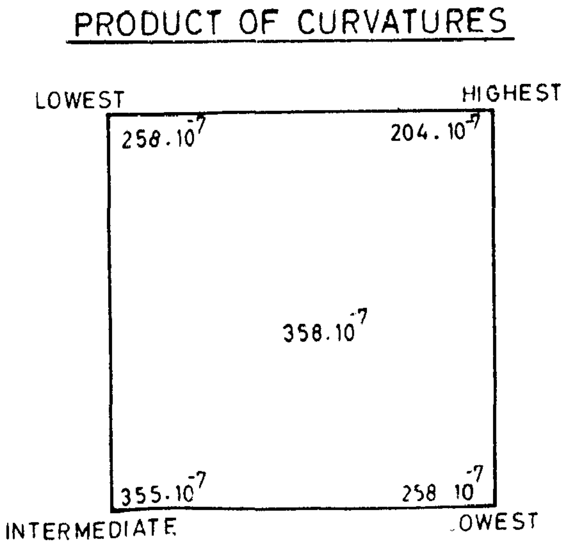

FIGURE 15

Thus the minimum value of the product of curvatu lies at the highest point endangering starting of buckling at that point (considering only numerical value)

Taking E for the concrete as $2x10^6$ p.s.i. and t = 4 ins.

$$p_{cr} = 0.15 \times 2 \times 10^6 \times 4^2 \times 204x10^{-7}$$

$$= 98 \text{ p.s.f.}$$

At the middle of shell, $p_{cr} = 98x\frac{358}{204} = 172$ p.s.f.

<u>Csonka's formula</u>

$$p_{cr} = 0.05\ Et^2 \ / \ R_1\ R_2$$

Hence p_{cr} for the highest point = 33 p.s.f. and for the middle of the shell = 57 p.s.f.

<u>Eric Reissner's Formula</u>

$$p_{cr} = \frac{2E}{\sqrt{3(1-\nu^2)}} \times \frac{t^2\ h^2}{a^4}$$

$$= \frac{2x2x10^6x4^2\ h^2}{\sqrt{3(1-0.15^2)} \times (112x12)^4} \text{ p.s.i.}$$

$$= 0.00166\ h^2 \text{ p.s.f. where 'h' is in inches.}$$

The formula has been derived for the hyperbolic paraboloid where one of the corners has been raised by height 'h' with respect to the other three which are at the same level, the equation being

$$z = \frac{h}{ab} xy = \frac{h}{a^2} xy \quad (\text{if } a = b)$$

In the present case the two opposite corners have been raised by 20 feet and 58.3 ft. respectively with respect to the other two which are at the same level, the equation being $z = \frac{h}{a^2} xy - (x+y) \tan\psi$ where, h =78.3 feet obtained by substituting the coordinates of some fixed point chosen on the shell.

Obviously, if only one point say E were 58.3 feet higher than the other three points at the same level, the buckling strength would have been lesser, since the effect of anticlastic curvature gets increased as soon as we raise the other corners by some amount. Since 'h' occurs in the numerator in all the formulae for buckling load, this increase in the value of 'h' is justified.

For h = 78.3, $p_{cr} = \left(\frac{78.3}{20}\right)^2 \times 95.6 = 1470$ psf.

<u>Anthony Ralston's Formula</u>

For h = 78.3 ft., $\frac{h}{t} = \frac{78.3 \times 12}{4} = 235 > 100$

Hence, we can directly use the formula

$$p_{cr} = \frac{4E}{\sqrt{12(1-\nu)}} \cdot \frac{t^2 h^2}{b^4}$$

which would give values exactly as above.

<u>A.Pflueger's formula</u>

$$\left[N_{xy}\right]_{cr} = 18.95 \frac{EI}{a^3} = \frac{q_{cr} \cdot a^2}{2h}$$

For $h = 78.3$ ft.

$$q_{cr} = \frac{37.9\ EI\ h}{a^5} = \frac{37.9 \times 2.10^6 \times 4.95 \times 10^6 \times 78.3 \times 12 \times 144}{1.567 \times 10^8 \times 112 \times 12^5} \text{ p.s.f.}$$

$$= 11660 \text{ p.s.f.}$$

<u>Dayaratnam's Formula.</u>

$$p_{cr} = 2E\left(\frac{h}{a}\right)^2 x \left(\frac{t}{a}\right)^2 x \sqrt{\frac{2}{3}\left(1 + \frac{2EI}{Da}\right)}$$

$$= \frac{h^2 t^2}{a^4} \sqrt{\frac{8}{3}\left(1 + 24\frac{I}{at^3}\right)}$$

$E = 2 \times 10^6$ p.s.i. $h = 78.3$ ft.

$a = 112 \times 12$ inches $= 1344$ ins.

$I = \frac{bd^3}{12}$ (neglecting steel)

$$= \frac{39 \times 115^3}{12} \text{ in}^4 = 4.95 \times 10^6 \text{ in}^4$$

$$D = \frac{E\,t^3}{12(1-\nu^2)}, \qquad \nu = 0.15$$

$$1 - \nu^2 = 1 - 0.0225 = 0.978$$

$$\therefore \frac{EI}{D.a} = \frac{4.95 \times 10^6 \times 12}{112 \times 12 \times 64} \times 0.978 = 676$$

$$P_{cr} = 51100 \text{ p.s.f.}$$

The values seem to be of only theoretical importance apparently, though it is possible that the assumed type of buckling may never take place for the present shell i.e. the shell along with the edge beams may not reach the critical unstable state of energy, failure having occurred much earlier due to other reasons.

These results can be tabulated as below (Table No.3)

Working load = 70 p.s.f.

Table No.3

No.	Author	Formula	Buckling load.	Remarks.
1.	H.Schmidt.	$p_{cr} = 0.15 \frac{Et^2}{R_1 R_2}$	98 psf.	Formulae are independent of 'h' and 'a'
2.	Csonka.	$p_{cr} = 0.05 \frac{Et^2}{R_1 R_2}$	33 psf.	
3.	Reissner	$p_{cr} = \frac{2E}{\sqrt{3(1-\nu^2)}} \cdot \frac{t^2 h^2}{a^4}$	1470 psf.	
4.	Ralston	$p_{cr} = \frac{2E}{\sqrt{3(1-\nu^2)}} \cdot \frac{t^2 h^2}{a^4}$ (For $\beta < 0.01$)	1470 psf.	$= \frac{t}{h}$
5.	A.Pfluger	$p_{cr} = 37.9EI \frac{h}{a^5}$	11660 psf.	It considers buckling of edge beam only.
6.	Dayaratnam and Gerstle	$p_{cr} = \frac{h^2 t^2}{a^4} \sqrt{\frac{8}{3}\left(1 + \frac{24I}{at^3}\right)}$	51100 psf.	

CHAPTER 4

MODEL TEST

4.1. Choice of Model Scale.

The design dimensions of the actual shell are quite large i.e. 112 feet by 112 feet, centre to centre of supports in plan with two opposite corners raised by 20 feet and 58.3 ft. respectively with respect to the other two. The shell thickness is 4 inches. Any size model could be tested, the limitations being the laboratory facilities available and the total amount in hand. A geometrically similar model was preferred so as to obtain a true picture of the failure and material selected also being the same as in prototype i.e. reinforced concrete.

" If we want to test an elasticity theory (14); model-materials, which follow the assumptions of this theory (Homogeneity, Isotropy, Validity of Hooke's Law) shall be chosen. For experimental design it will sometimes be sufficient to know the nature of deformations, for such purpose more materials will be suitable.

Two groups may be distinguished for the models. One, when we primarily copy the form of structure on a reduced scale and the other for which in addition a reproduction of the properties of material of the structure is carefully achieved. In the second group, the properties of the materials of the structure should be reproduced by those of the model material and this reproduction should also hold true under increasing load into collapse-condition. As a rule this aggreement in behaviour between the model and the future structure is judged by comparing the stress-strain diagrams of the model materials to the materials to be used. This transition is specially of value for shells of reinforced concrete. Not only a check on the stress-distribution will be the goal, the concurrent phenomenae like crack-formation, deflection, yielding of the reinforcement are equally important. For a good agreement between model and real structure the stages in loading in which these phenomenae occur should coincide with reality.

For such a thorough and realistic investigation the different particles of the concrete should be reduced in size according to the scale involved. If applied to the aggregates (gravel, sand and cement) it will lead to a micro-concrete. However, a substitute for a smaller grained cement can hardly be found. It will thus be possible to reduce to a scale of about 1:10. A limit is also set by the minimum thickness of the shell membrane of the model, which should not be much lesser than about 10 mm. on account of reasons of manufacturing. Often models of reinforced mortar are taken to be sufficient."

A scale-factor of 9.33 was used, which was close to the above recommended value thus requiring a size of 12 ft. by 12 ft. centre to centre in plan. This dimension was adopted because the supporting beams of the test-frames were already fixed at 12 feet centres. The reinforcement was taken in the nearest size available equal to the diameter geometrically reduced and spacing was slightly modified accordingly. The size of the coarse aggregate was also reduced in the same proportion and the finest available sand was used as the fine aggregate. The approximate strength was checked upto be the same as provided in the design of the prototype by means of seven days compression tests. On this basis the mix proportion had to be taken as 1:1:2 instead of 1:1.5:3 as in the original design after several trials, since the strength of concrete and the sizes of aggregate were considered more important to be tallying than the proportion of mix.

There was not much choice for the strength of steel, since the only available quality in the vicinity of the required size (i.e. 2 m.m.) had to be used. However, the average strength was not much different, though the individual test-specimen showed variations in the stress-strain curve and ultimate load in tension upto the extent of ± 50%.

For greater accuracy and better interpretation all these factors are very important, the variations may cause localised effects. However, due to shortage of time it was not possible to wait much longer and for all the practical purposes of the thesis the conditions are taken to be representing the true prototype ones.

The reinforcement in the proto-type as well as the model was placed along the ruling lines instead of the diagonal directions of the direct stresses for the reasons of convenience and better accuracy in placement, quick work and overal economy.

4.2 <u>Model Design</u>

Prototype dimensions centre to centre in plan

= 112 ft x 112 ft.

Model dimensions = 12 ft. x 12 ft.

∴ Scale factor = 9.33

Table No.4.

ORDINATES OF THE TOP SURFACE POINTS OF THE SHELL MODEL

x \ y	0	0.857	1.75	2.57	3.43	4.28	5.14	6.0
0	5.14	4.98	4.83	4.68	4.53	4.38	4.23	4.07
0.857	4.98	4.88	4.77	4.65	4.54	4.43	4.33	4.22
1.715	4.83	4.77	4.68	4.68	4.55	4.48	4.41	4.34
2.57	4.68	4.65	4.68	4.58	4.56	4.53	4.51	4.48
3.43	4.53	4.54	4.55	4.56	4.58	4.59	4.61	4.63
4.28	4.38	4.43	4.48	4.53	4.59	4.61	4.72	4.78
5.14	4.23	4.33	4.41	4.51	4.61	4.72	4.82	4.92
6.00	4.07	4.22	4.34	4.48	4.63	4.78	4.92	5.07
6.85	3.92	4.11	4.27	4.46	4.78	4.84	5.02	5.22
7.72	3.77	4.00	4.21	4.44	4.67	4.90	5.13	5.37
8.57	3.61	3.89	4.14	4.42	4.69	4.96	5.24	5.51
9.42	3.46	3.78	4.07	4.39	4.70	5.02	5.34	5.65
10.28	3.31	3.67	4.00	4.37	4.72	5.08	5.44	5.80
11.14	3.16	3.55	3.94	4.34	4.79	5.14	5.54	5.94
12.00	3.00	3.44	3.87	4.31	4.76	5.20	5.64	6.08

Table continued on next page.

Table No. 4 Continued.

x \ y	6.85	7.72	8.57	9.42	10.28	11.14	12
0	3.92	3.77	3.61	3.46	3.31	3.16	3.00
0.857	4.11	4.00	3.89	3.78	3.67	3.55	3.44
1.715	4.27	4.21	4.14	4.07	4.00	3.94	3.87
2.57	4.46	4.44	4.42	4.39	4.37	4.34	4.31
3.43	4.65	4.67	4.69	4.70	4.72	4.74	4.76
4.28	4.84	4.90	4.96	5.02	5.08	5.14	5.20
5.14	5.02	5.13	5.24	5.34	5.44	5.54	5.64
6.00	5.22	5.37	5.51	5.65	5.80	5.94	6.08
6.85	5.39	5.59	5.78	5.97	6.15	6.34	6.52
7.72	5.59	5.82	6.05	6.28	6.51	6.74	6.97
8.57	5.78	6.05	6.32	6.60	6.86	7.14	7.41
9.42	5.97	6.28	6.60	6.92	7.23	7.54	7.86
10.28	6.15	6.51	6.86	7.23	7.58	7.94	8.30
11.14	6.34	6.74	7.14	7.54	7.94	8.34	8.74
12.00	6.52	6.97	7.41	7.86	8.30	8.74	9.19

Table concluded.

Thickness of main shell body $= \frac{4}{9.33} = \frac{7"}{16}$ (say)

The coordinates are given in the accompanying table No.4 , where the relative heights are to be considered , since actual heights depend upon columns.

Main reinforcement $= \frac{0.47}{9.33^2}$ sq.ins. per 9.33 ft.

$= \frac{0.47}{9.33}$ sq.ins. per ft.

Spacing of 2 m.m. dia ($\frac{1}{12.7}$ ins) wires

$= \frac{12}{4x12.7^2} x \frac{9.33}{0.47}$

$= 1\frac{1}{8}$ inch c/c (say)

Hence (144/ $1\frac{1}{8}$) i.e. 128 wires will be placed in each direction along the ruling lines at the mid-depth of the shell.

Thickening of the shell will be done in $\frac{14}{9.33}$ i.e. 1.5 ft. near the edges all around, which should be $\frac{6}{9.33}$ inch. To accommodate two layers of the mesh conveniently 3/4 inch. thickness will be provided at the edges in 1.5 ft. width uniformly. Extra mesh of 2 m.m. wires at $1\frac{1}{8}$ in.c/c will be provided at top all along in this thickened portion.

Edge Beams

Section will be $\frac{39}{9.33}$ ins x $\frac{115}{9.33}$ ins i.e. 4¼ insx12½ ins.

Beams EP and EP'

Length = $\frac{126.5}{9.33}$ = 13.56 ft. c/c.

Overall length = 13 ft. 6¾ ins. + 4¼ ins.

= 13 ft. 11 ins.

Steel area at top or bottom = $\frac{33x1.77}{9.33x9.33}$ = 0.447 sq.ins.

Since bond is no problem , we can use thicker bars, say ¼ inch. dia.

∴ Number of ¼ inch. dia. bars = $\frac{0.447}{0.449}$

= 10

10 bars each at top and bottom will be provided in two layers, 5 in each with clear top cover and clear distance between two layers as ¼ inch. Further 2 bars on each side of the beam will be provided equidistant from the centre to take up the torsion.

Inner layers will be curtailed at 2¼ ft. from ends at top and bottom both.($\frac{1}{8}$ inch dia.)-Double-legged stirrups will be provided at 8 ins. c/o throughout.

<u>Beams OP and OP'</u>

These will have same provisions as above except that their inner layers will be curtailed at 2 ft. from ends.

$$\text{Length} = \frac{114}{9.33} = 12.24 \text{ ft. c/o}$$

$$\text{Overall length} = 12 \text{ ft } 2\tfrac{7}{8} \text{ ins.} + 4\tfrac{1}{4} \text{ ins.} = 12 \text{ ft. } 7\tfrac{1}{8} \text{ ins.}$$

<u>Ties</u>

$$\text{Total area} = \frac{200}{9.33^2} = 2.3 \text{ sq.ins.}$$

4 bars 1 inch. dia. will be provided and jointing at the corner shall be done for proper anchorage by means of $\frac{1}{8}$ inch. dia. stirrups as shown in the accompanying Figure (No.16), the ties being taken inside the beams and embeded in proper length.

<u>TIE BARS</u>

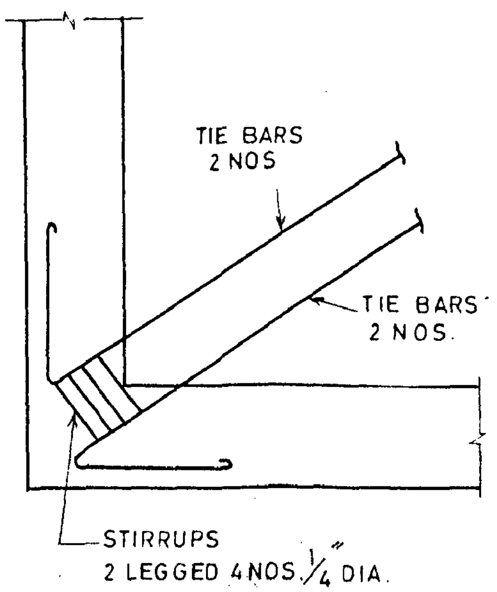

FIGURE-16

Design of Columns.

Approximate load @ 70 lbs/sq.ft. on slab

= 12x12x1.06x70 = 10700 lbs.

Approximate weight of beams

= 2x(13.56+12.24)x4.25x12.5

= 2740 lbs.

Total load = 13440 lbs.

Weight on one column

= 6720 lbs.

Allowing for unknown ultimate load of the shell (since load-factor may be even 7 or 8 and the normal factor of safety of 3 may not suffice), the failure of supports is in the least desirable.

Let the columns be designed for a load of $\frac{6720x8}{3}$ i.e. 17920 lbs. For 1:6 cement and sand mortar in brick masonry,

Minimum size required = $\frac{18000}{300}$ = 60 sq.ins.

Further providing for unequal distribution of the load as a whole on the columns or eccentricity due to inaccuracy of construction as well as the self-load of columns and pedestals the column sizes in the model have been provided as $13\frac{1}{2}$ ins x 18 ins, the former dimension being limited by the width of supporting bottom-beams of the loading frame in the test hall. This would also omit the danger of buckling of columns themselves, one of them being 8 ft. high.

R.C.C. Pedestals.

For uniform load distribution over the columns, pedastals of reinforced concrete monolithic with the shell were cast below the four corners joining the two beams.

The design was done as for the simple foundations and need not be given here.

Loading

Because of large slopes of the surface, a uniform loading by means of bricks or blocks was not possible. For buckling tests, pneumatic pressure loading is the best but this could not be arranged. Hence uniformly distributed load was approximated(Load over the shell surface)by applying uniform load at 16 uniformly spaced points of the shell surface. Load applied by means of one jack was transferred to the 16 points uniformly through a system of beams simply supported at ends.

The bottom-most beams rested over brick columns 9 ins x 9 ins. in section.

The loading system (beams and brick columns) were designed to take up a total load of 30 tons, though the design-load is about 4.7 tons only. The size of brick column-bases was determined by shear and punching load capacity of the thin curved shell-surface.

4.3 Buckling Loads in the Model.

Since geometrically similar model has been adopted, the uniformly distributed load intensity per unit area of the shell surface remains the same in the model and prototype. The total buckling load on the shell can now be calculated easily. (Table No.5)

$$\text{Area} = 1.06x(11.646)^2 = 143.7 \text{ sq.ft.}$$

The intensities of the loads have been calculated in Chapter 3, article 3.5 according to various theories.

Table No.5

No. Author	Load intensity in p.s.f.	Buckling load in tons (Total over surface)
1. H.Schmidt.	98	6.28
2. Csonka	33	2.12
3. Reissner	1470	94.30
4. Ralston	1470	94.30
5. A.Pfluger	11660	748.00
6. Dayaratnam and Gerstle	51100	3280.00

4.4 Construction Details.

The important points of construction including the difficulties experienced and suggestions for future work are given below:-

1. Although the shuttering consists of straight planks, smoothening of joints between planks was necessary because the thickness of the shell was only $\frac{7}{16}$ in. Moreover the timber available was not fully seasoned and got warped by the time casting was done. The effect of such variations is far from negligible due to the change in geometry specially because the thickness is so small. The straightness of the ruling lines is all the more important as the reinforcement wires are very thin. Due to warping the original beam width of $4\frac{1}{4}$ ins. was reduced to $3\frac{1}{2}$ ins. at places and beams became curved in plan. Hence, plywood or some suitable hard-board must be used instead of ordinary chir wood. Fully seasoned deodar or teak wood may also be used.

2. Battens are very necessary along the curved surface at close intervals below the shuttering planks and should be supported by props at close intervals other-wise the shuttering becomes very flexible and tries to take its own deformed shape under self-load and persons working above it. It was found that shuttering of edge beams at

the corner i.e. the highest point shifted inwards towards the centre of the shell. As a result the load on column would have become eccentric. Therefore, the column was widened on the inner side so as to make the beam loads central on it.

EXTENSION OF COLUMN

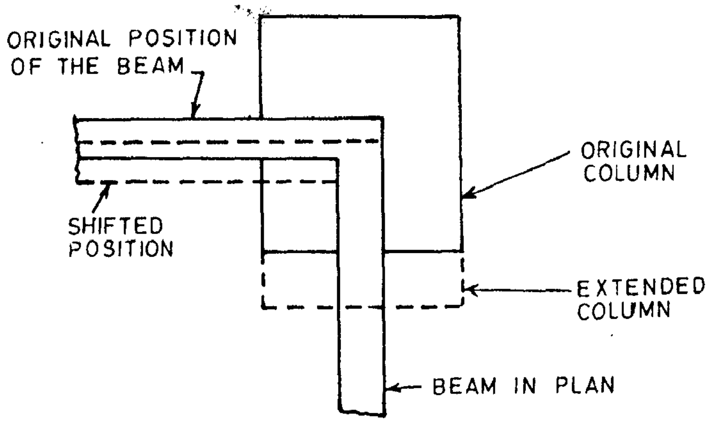

FIGURE_17

Figure No.18- Bottom View of Shuttering.

3. The surface of the shell shuttering was prepared in the following manner. After the planks were fixed, planing was done to give a uniform surface and the holes and crevaces were packed with timber pieces. Putin was applied to fill in the gaps completely which was prepared by mixing chalk powder in sares. A cement and sand 1:5 mortar layer was applied for further uniformity over which tar paper pieces were stuck by glue to check water

of concrete rinsing through timber.

4. The thin wires took considerable time in straightening them, as a kink of 1/8 inch would cause 30% alteration in the effective depth of the shell, which could very easily occur in the lengths of 12 to 14 feet.

5. In attempting to reduce the beam reinforcement size in the ratio of the scale factor, the small size created lot of difficulty, since $1\frac{1}{2}$ ins. to 2 ins. diameter bars are used in prototype but in model even 1/4 inch diameter bars become inconvenient in 12 ft. to 15 ft. long beams. Hence, thicker bars should have been used keeping the total area as calculated by dimensional analysis.

6. At corners after the placing of ties it was difficult to accommodate the heavy beam reinforcement along with them at proper spacing with proper cover due to overall width being only about 4 ins. Hence, what can be done is to prepare shuttering without the sides of the beams , place the reinforcement and thenfix the sides of beam shuttering.

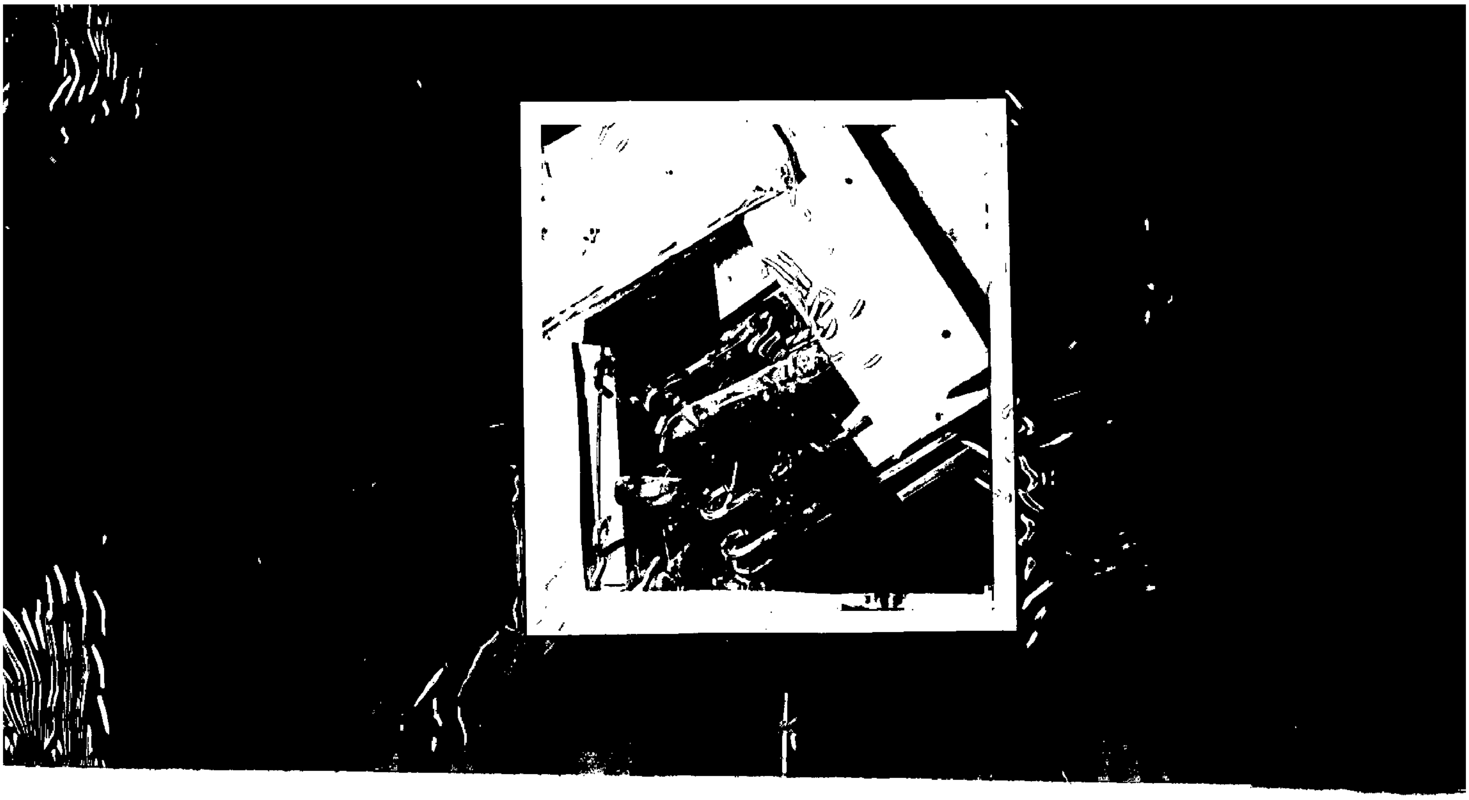

Figure No.19- Reinforcement at corners.

7. The 2 m.m. dia. wire mesh had to be soldered at close intervals since binding wire would increase the thickness. Sand-papering and application of hydrochloric acid on the wires had to be done so that solders became effective. Further tying was also difficult since the wires used to slip on the sloping surface and soldering all around the edges held them better.

Very small concrete blocks of required sizes at different points depending upon the cover desired were stuck to the tar paper surface by glue so as to check their sliding over the curved surface.

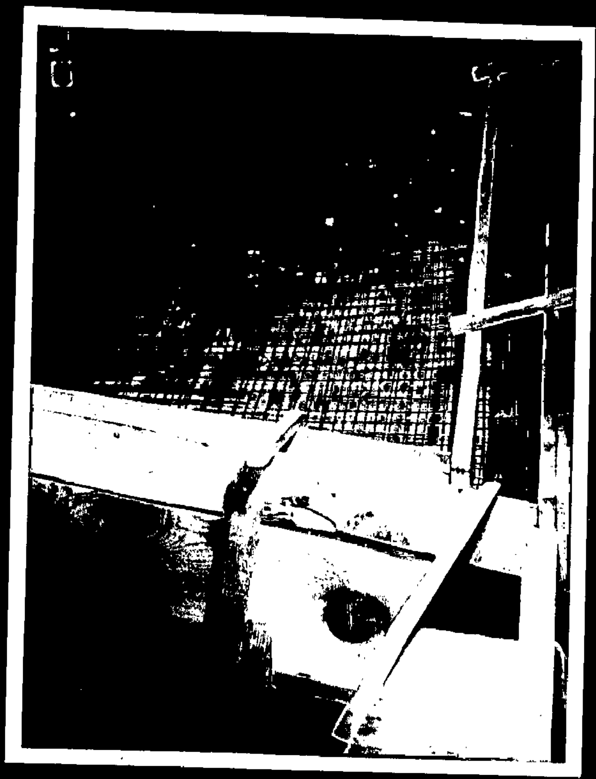

Figure No.20 - View of Reinforcement

8. Bending of 1 in. dia tie rods so as to accommodate the bends and hooks within the small beam width was also a difficult task. Thinner ties also are not advisable, since the number would become too large to be accommodated within the beam-depth. The ties must be bent and placed in position prior to the fixing of beams side-shuttering. The piercing through the slab has to be done carefully.

Proper length of embedment of ties was provided in beams (two on either side) which were tied by stirrups as already shown in Figure No.16.

Welding the straight ties at ends with the bents prepared earlier would be more convenient and their placing can be done easily after the shuttering has been prepared completely (Figure No.21).

BETTER ARRANGEMENTS FOR TIES

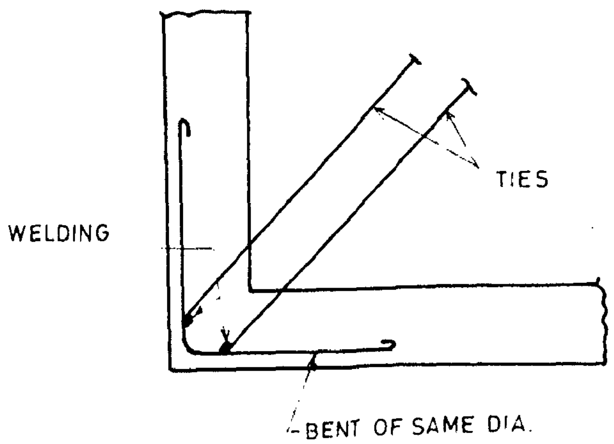

FIGURE 21

9. Monolithic R.C. pedestals were provided over the brick columns below all the four shell-corners for uniform distribution of the load. The pedestals and the columns must be over safe so as to guard against the high unknown

range of load-factor, unequal load-distribution on the columns and the eccentricities introduced at various stages, so that the test on the shell may be carried to its ultimate without any premature failure in the auxiliary members such as the supports.

The columns and bases in the present experiment were designed on the basis of a load-factor equal to 8. Though the load-factor actually found was 4 only, yet one of the pedastals at the topmost column had started lifting up towards the end of experiment.

Figure No.22 - Shell ready for concreting

10. Due to very small thicknesses of slab ($\frac{7}{16}$ inch) and the reinforcing wire (2 m.m.) the size of coarse aggregate had to be restricted to 2 m.m., also as required according to model scale. Considerable time was consumed in procuring this sand by sieving from various ballast

stacks. Approximate strength was judged by casting and testing 4 inches cubes for seven days strength. A reasonable mix was achieved only after three trials hence this must be done invariably in all cases of very thin aggregates, since there is a large variation in their strengths with reduction of size.

11. Due to high accuracy required for small shell thickness, movements over the shuttering as well as the slab after casting have to be avoided. Moreover it is very difficult even to stand on the surface due to large slope. Therefore, a frame work of pipes was used, which were clamped and tied with ropes to each other and outside girders. The workers could move over the planks placed suitably over them with the help of ropes.

After removal of shuttering persons need moving about the shell for pasting strain gauges, placing the loading arrangement and casting loading columns and taking observations, which cause live loads and set up vibrations in the shell. Therefore an elaborate stepping system must be made independent of the shell so that the observations are not disturbed. The steps must be quite close to the surface so that they may be utilised safely and climbing over shell surface is not required.

12. In absence of the arrangement of applying uniformly distributed load pneumatically the load was applied at 16 points uniformly placed over the shell surface. Small bases of 9 in. x 9 in. section with their top horizontal were cast simultaneously with the shell and small steel bar pieces of $\frac{1}{4}$ in. dia. were inserted through them in the shell to act as dowels and check shearing off . Later brick columns of 9 inx9 in. size were constructed over them, such that their tops were all at the same level.

Girders were placed simply supported, each transferring the load applied at its mid point to the lower two beams at its ends placed below it.

Small flats with 3/8 inch diameter bars welded over them were used to avoid moments and allow rotations at all such supports to the loading beams thus acting as rollers.

The beams must be designed for a total load larger than that which is actual expected to come over them. Careful consideration should be given to the lateral stability of the beams, hence that of the whole loading arrangement, otherwise the whole skeleton of tiers

THE SIXTEEN POINTS LOADING ARRANGEMENT

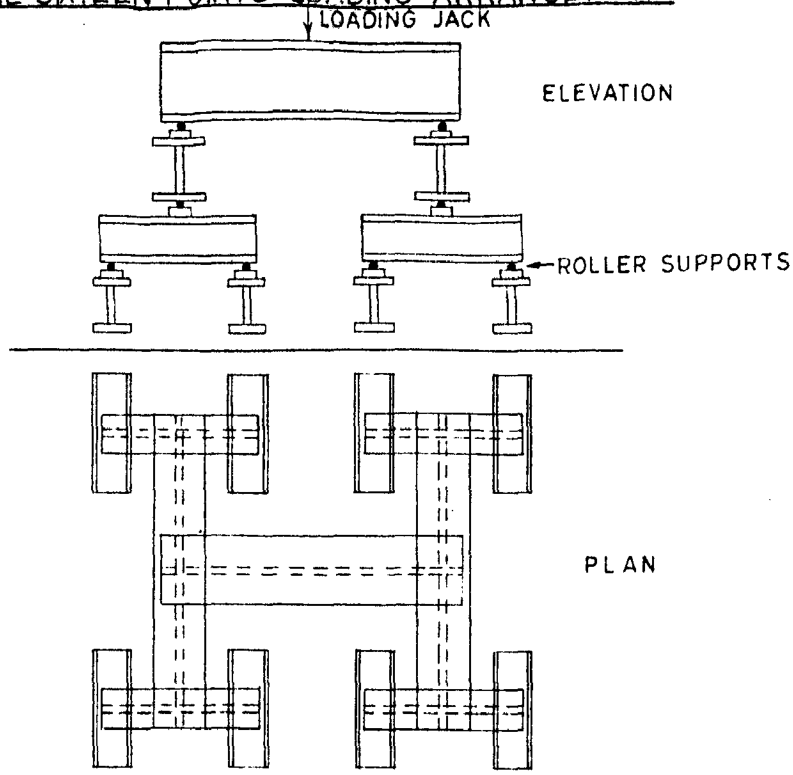

FIGURE_23

of beams may collapse suddenly and accidents may occur. Stiffeners are essentially required on beam web at points of concentrated loads and reactions.

However the method of replacing uniformly distributed load by many concentrated loads is not accurate enough. In thin shells like the one tested localised effects become large. The effects are even more adverse in the study of buckling behaviour where the stiffness properties may also get modified considerably because of loading columns. For the purpose of present thesis the load applied has been taken as uniformly distributed and the stiffness properties assumed unchanged.

Figure No.24 <u>Arrangement of Loading-test</u>

13. The space between the shell-surface and the bottom of the loading-frame girder must be checked in the beginning to accommodate all the loading beams, jack and proving ring or a load cell of the required capacity. The cell or the ring must be caliberated and checked in advance to avoid delay at the eleventh hour after the heavy loading system has been placed on the shell.

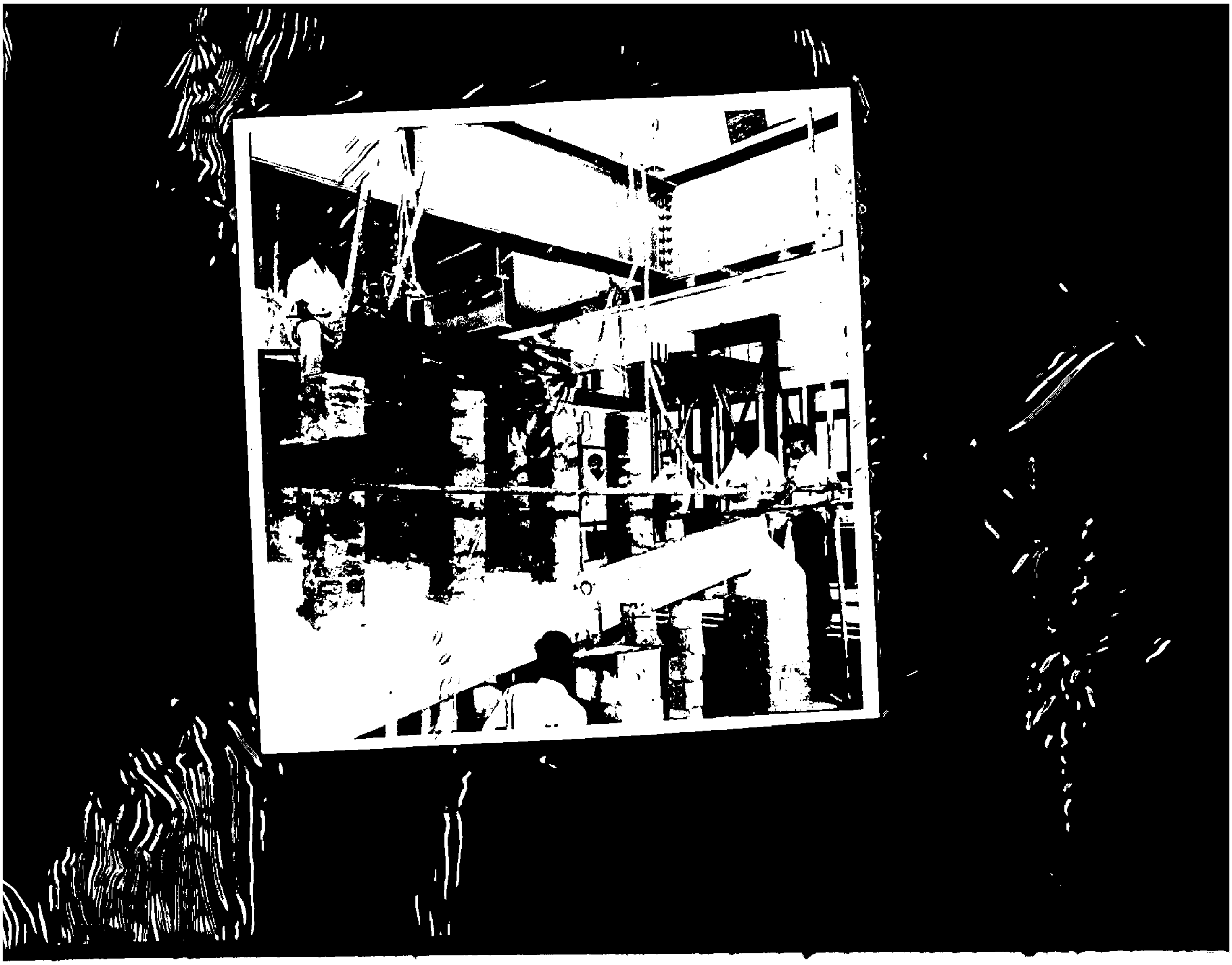

Figure No.25. Test in Progress.

14. Strain-gauges(manufactured in Roorkee "Rohit Gauges") were used for the strain-measurements. Wooden blocks of slightly larger size were left in the cover for the reinforcement bars, where strain was to be measured while casting, which were taken out later. Copper foils were used over the concrete surface for better results and protection from moisture.

In case curing is to be continued even after pasting the strain-gauges due to shortage of time, some water-proof compound must be applied over them. A water-repellent compound (No.514) is available with "Rohit" of Roorkee, which however could not be tried in the present experiment.

15. Test-specimens of concrete mixes used e.g. cylinders, beams, cubes, tension-specimen etc. must be cured under the same conditions as the shell model at the same place.

16. Safety arrangement must be made below the shell for the people to take the dial gauge and deformeter readings there. Planks can be placed over dry brick columns raised upto slightly below the bottom of the shell as a simple device. This would allow the people to record observations without any fear and danger of a sudden collapse.

17. Dial gauges were fixed at various points with their magnetic bases attached to steel plates placed over 6 ins. square columns of concrete cubes in 1:6 mortar. Bricks may also be used. It is better to construct them early so as to have an idea of the space available for movement and arranging safety precautions against any possibility of a sudden collapse.

LOCATIONS OF LOADING COLUMNS AND MEASURING GAUGES

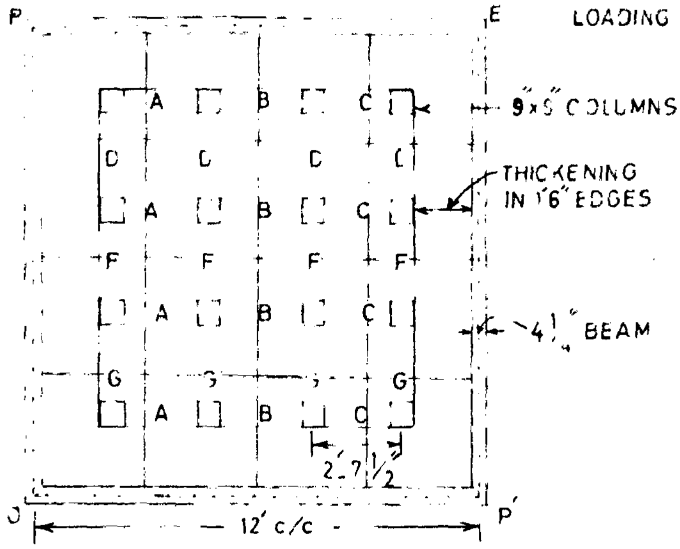

LINES A, B, C, D, E, F, G WERE DRAWN FOR CONVENIENCE OF STUDYING CRACK PATTERN

POSITIONS OF STRAIN GAUGES

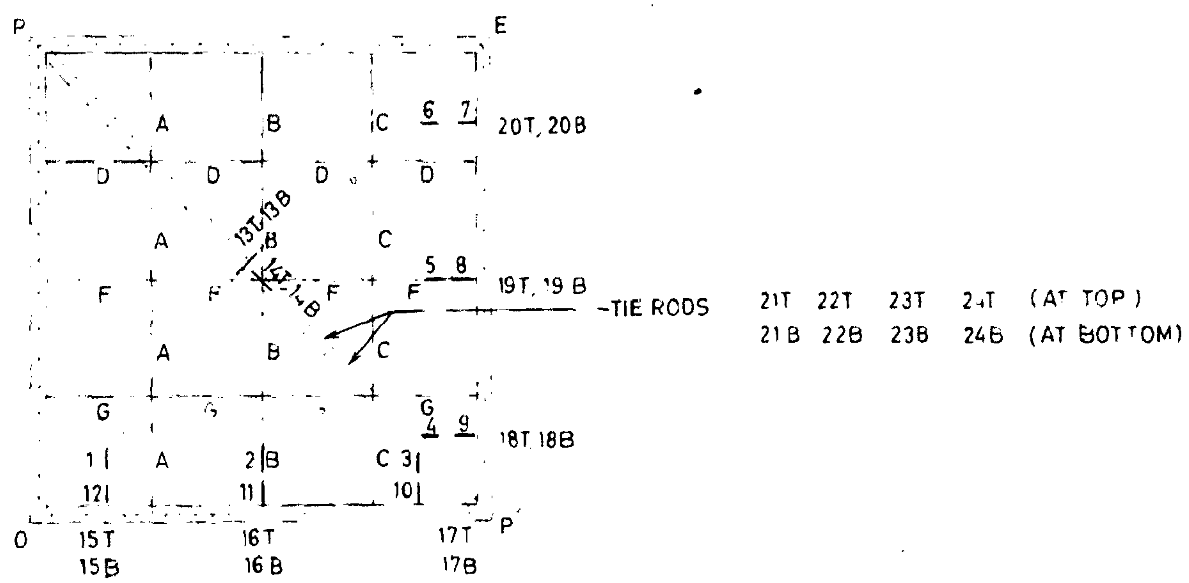

POSITIONS OF DIAL GAUGES

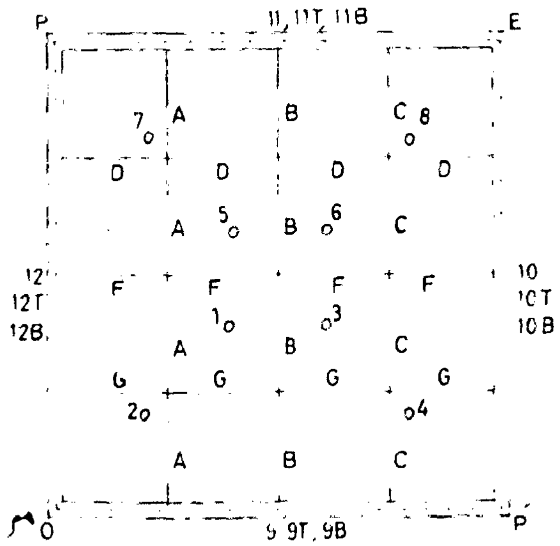

9, 10, 11, 12 - FOR VERTICAL DEFLECTIONS

9T 10T 11T 12T - FOR HORIZONTAL DEFLECTIONS AT TOP OF BEAMS

9H, 10H, 11H, 12H. FOR HORIZONTAL DEFLECTIONS AT BOTTOM OF BEAMS

FIGURE - 26

18. The dial-gauges, strain-gauges and deformeter readings were started only after the loading arrangement had been placed on the shell. Thus in addition to the dead load about 2 tons more had already been borne by the shell, when the strains or deflections were started to be taken. This load was added to the load applied by jack to get the total load. To get the strains and the deflections therefore the instruments must be fixed up before the removal of shuttering and even dead weight observations recorded for a true picture of the shell-action.

4.5. Observations and Results.

Stress-Strain Curves.

The cylinder-specimens of the concrete used in pedastals and main body of the shell were tested on the same day as the testing of shell on 200 ton compression machine and the stress-strain curves are given in Figure No.27.

The stress-strain curves of the 2 m.m. diameter wires and $\frac{1}{4}$ inch. dia bars were also obtained and are given in Figure No.28.

Cube Strength.

The results of the cube tests are tabulated as below (Table No.6):

Cube size : 6 inches x 6 inches x 6 inches

Table No.6

Concrete used in	No.	Load at failure	Average Load	Crushing Strength.
Pedastals	1	74.2 tons	64.77 tons.	1.8 T/in^2 or 4000 p.s.i.
	2	63.60 tons		
	3	56.50 tons		
Main Shell	1	61.50 tons	58.45 tons.	1.622 T/in^2 or 3640 p.s.i.
	2.	54.30 tons		
	3.	59.55 tons		

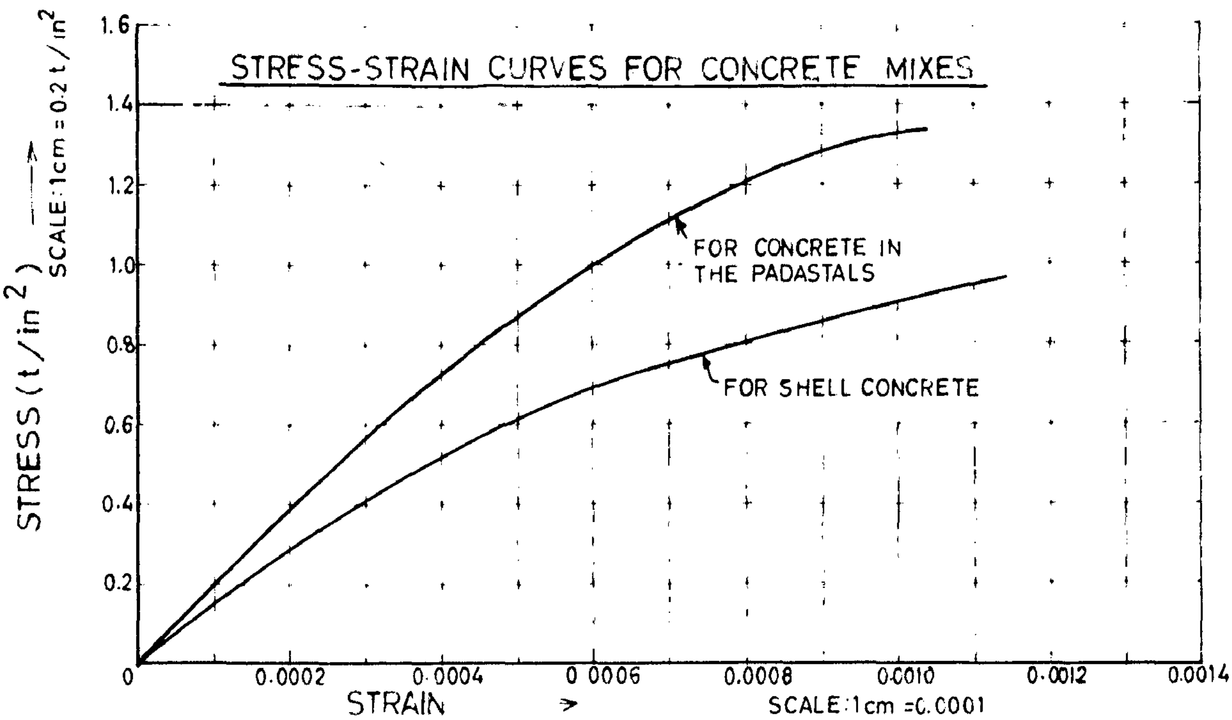

FIGURE_27

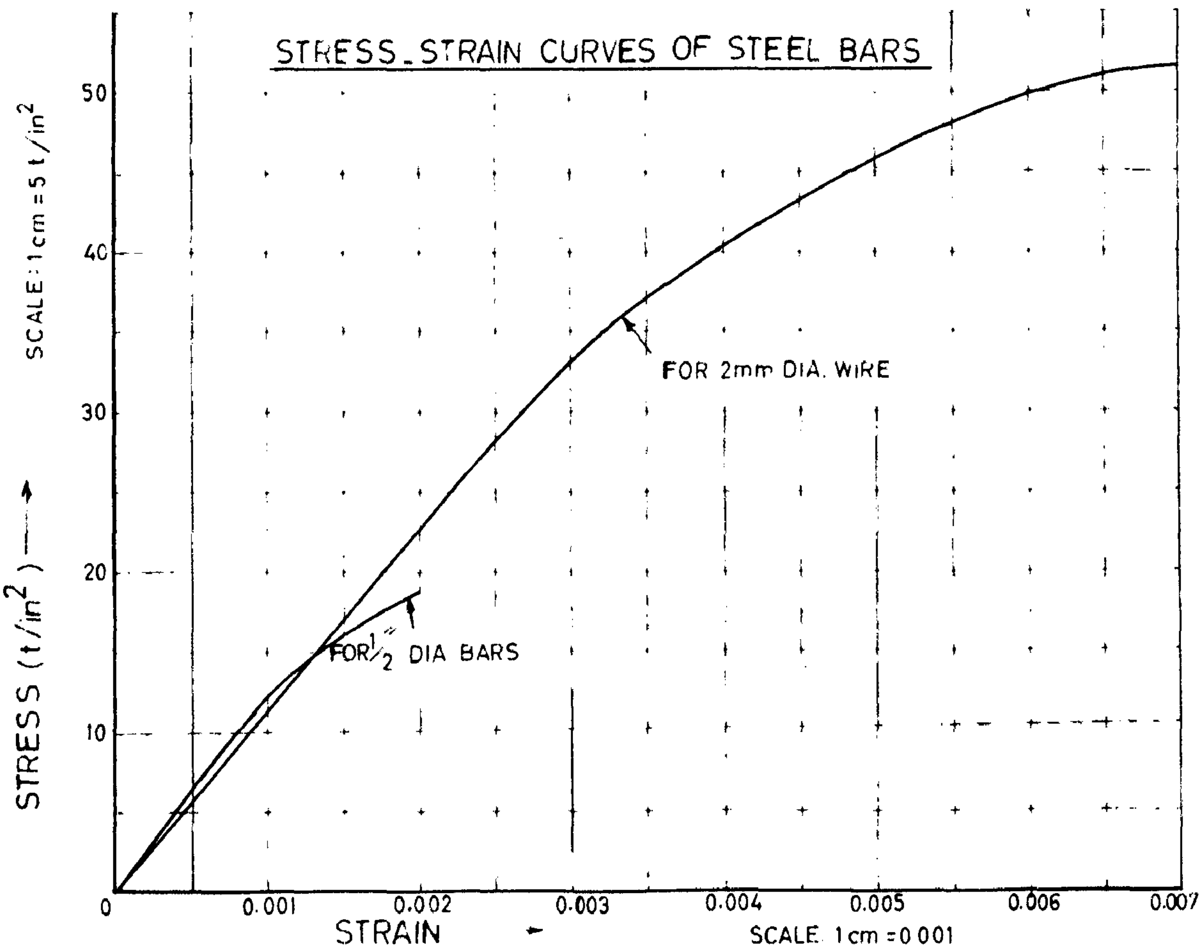

FIGURE_28

Loading Test.

Weight of loading columns and beams = 2.02 tons
= 2 tons(say)

Arrangements to measure the deflections and strains were made at the points as shown in Figure 28. Strain observations were taken by electrical resistance strain-gauges as well as Huggen-burger extensometer but the order of the deformeter readings varied by large amounts and being unreliable they were completely neglected.

The deflections and strains at various points with the increments of total load on the shell have been tabulated as below:-

Table No.7 - Vertical deflections of beams and slab with respect to the total load at various points.

Table No.8 - Lateral deflections in beams.

Table No.9 - The average deflections and rotations in beams have been calculated.

Table No.10 - Strains in concrete.

Table No.11 - Strains in steel.

The load deflection curves have been plotted in Figure No.29.

Cracks and Failure.

Cracks visible to the naked eye began to appear at a load of 4 tons. The bottom surface of the shell was

Point No.	Shell								Beams			
Total load in Tons.	1	2	3	4	5	6	7	8	9	10	11	12
0.0	0.000	0.000	0.000	0.000	0.000	0.000	0.0000	0.0000	0.0000	0.0000	0.0000	0.00000
0.5	0.020	0.037	0.020	0.009	0.000	0.030	0.0005	0.0100	0.0003	-0.0010	[illegible]	0.00000
1.0	0.033	0.050	0.055	0.010	0.003	0.056	0.0000	0.0305	0.0010	-0.0015	-0.0015	0.00040
2.0	0.178	0.171	0.116	0.031	0.015	0.106	-0.0015	0.1020	0.0015	-0.0020	-0.0015	0.00025
3.0	0.410	0.210	0.150	0.049	0.051	0.190	-0.0140	0.1470	0.0025	-0.0025	-0.0015	0.00060
4.0	0.420	0.265	0.316	0.056	0.065	0.235	-0.0160	0.2060	0.0010	-0.0040	-0.0015	-0.00160
5.0	0.435	0.323	0.410	0.067	0.127	0.330	-0.0170	0.4040	-0.0020	-0.0050	-0.0030	-0.00310
7.0	0.522	0.413	0.630	0.130	D.G. out of order	0.550	-0.0235	0.7210	-0.0055	-0.0110	-0.0010	-0.00710
10.0	0.010	Greater than 0.5"	0.023	0.263		0.779	-0.0316	0.0160	-0.0175	-0.0200	-0.0015	-0.01210
13.0	D.G. removed	D.G.removed.	D.G.removed.	D.G.removed.		D.G.removed.	D.G.removed	D.G.removed.	-0.0365	-0.0325	-0.0015	-0.02200
16.0									-0.0450	-0.0320	Gauge out of contact	-0.03360
17.4												-0.03560
19.4		COLLAPSE		OCCURRED								

Table No.14 LATERAL DEFLECTIONS IN INCHES (T=Top, B=Bottom)

Point No. Total load in tons.	9T	9B	10T	10B	11T	11B	12T	12B
0.0	0.00000	0.00000	0.0000	0.0000	0.0000	0.0000	0.0000	0.0000
0.5	-0.00050	0.00000	-0.0055	-0.0035	0.0000	0.0030	0.0005	0.0000
1.0	-0.00120	0.00000	-0.0070	-0.0045	0.0000	0.0055	0.0005	0.0000
2.0	-0.00160	0.00000	-0.0115	-0.0075	0.0000	0.0035	0.0036	0.0016
3.0	-0.00250	0.00050	-0.0135	-0.0100	0.0060	0.0100	0.0105	0.0030
4.0	-0.00325	0.00050	-0.0155	-0.0105	0.0100	0.0220	0.0125	0.0165
5.0	-0.00205	0.00070	-0.0125	-0.0140	0.0230	0.0320	0.0275	0.0235
7.0	0.00345	0.00270	-0.0235	-0.0275	0.0305	0.0420	0.0433	0.0403
10.0	0.01090	0.01035	-0.0445	-0.0400	0.0400	0.0555	0.0600	0.0627
13.0	0.01540	0.01920	-0.0765	-0.0750	0.0525	0.0620	0.0861	0.0313
16.0	0.01440	0.01045	-0.0935	-0.1100	0.0550	0.0750	0.1091	0.1006
17.4					0.0502	0.0875	0.1100	Gauge out of order
19.4	COLLAPSE	OCCURRED						

Table No.20: STRAIN IN CONCRETE (Tensile +ve, Compressive -ve)

Points / Load in tons.	1	2	3	5	11
0	0	0	0	0	0
0.5	-0.000002	-0.000002	-0.000003	0	-
1.0	-0.000003	-0.000005	-0.000012	0.00002	0.0000100
2.0	-0.000007	-0.000011	-0.000025	0.00005	-
3.0	-0.000010	-0.000020	-0.000037	0.00005	0.0000205
4.0	-0.000013	-0.000024	-0.000050	0.00006	-
5.0	-0.000010	-0.000030	-0.000060	0.00009	0.0000005
7.0	-0.000010	-0.000030	-0.000060	0.00013	0.0000400
10.0	-0.000022	-0.000030	-0.000060	0.00000	0.0000000
13.0	-0.000024	-0.000020	-0.000050	0.00006	0.0001200
16.0	-0.000026	-0.000040	-0.000061	0.00003	-
17.4	-0.000027	-0.000040	-0.000050	0.00001	-
10.4	Collapse occurred.				

TABLE No.11- STRAINS IN STEEL (tensile strain=+ve) (compressive strain =-ve)

Point Lo ad tons	15T	15B	16T	16B	17T	17B	18T	18B	19T
,0	0.0000	00.00000	0.00000	0.0000	0.0000	0.00000	0.00000	0.00000	.0000
.5	0.0001	0.00000	-0.00326	-0.0059	0.0000	0.00000	0.00000	0.00000	.0040
.0	0.0005	0.00000	-0.00326	-0.0066	-0.0010	0.00000	0.00002	0.00000	.0074
.0	0.0012	0.00000	-0.00365	-0.0050	-0.0015	0.00010	0.00004	-0.00001	.0094
.0	0.0016	0.00000	-0.00350	-0.0046	-0.0020	0.00020	0.00144	-0.00001	.0094
.0	0.0020	-0.00004	-0.00347	-0.0016	-0.0002	0.00024	0.00420	-0.00001	0.013(
.0	0.0020	-0.00004	-0.00311	-0.0012	-0.0002	0.00030	0.00204	-0.00001	0.009
.0	0.0020	-0.00008	0.00000	-0.0010	0.0008	0.00037	0.00204	-0.00001	0.005
.0	0.0022	-0.00012	0.00020	-0.0008	0.0015	0.00035	0.00204	0.00000	0.004
.0	0.0037	-0.00016	0.00034	-0.0004	0.0068	0.00035	0.00004	0.00002	-
.0	-	-0.00017	-	-	-	0.00035	-	0.00006	-
.4	-	-0.00047	-	-	-	0.00034	-	0.00015	-
',4	-	Collapse load.							

Table continued on next page.

Table 11- continued.

Point No. / Load in tons	19B	20T	20B	21T	22T	23B	24T	24B
).0	0.00000	0.0000	0.00000	0.00000	0.00000	0.00000	0.00000	0.00000
).5	0.00000	0.0002	0.00000	0.00002	0.00004	0.00001	0.00003	0.00000
l.0	-0.00001	0.0012	0.00000	0.00004	0.00006	0.00002	0.00005	0.00000
l.0	-0.00002	0.0017	0.00050	0.00006	0.00009	0.00005	0.00010	0.00003
l.0	-0.00002	0.0027	0.00090	0.00012	0.00012	0.00006	0.00014	0.00004
l.0	-0.00002	0.0037	0.00600	0.00015	0.00018	0.00009	0.00018	0.00006
l.0	-0.00002	0.0030	0.00250	0.00010	0.00021	0.00013	0.00022	0.00007
'.0	-0.00003	0.0029	0.00150	0.00030	0.00025	0.00019	0.00030	0.00012
).0	-0.00004	0.0022	0.00105	0.00041	0.00028	0.00020	0.00041	0.00021
).0	-0.00005	0.0022	-	0.00051	0.00030	0.00027	0.00051	0.00030
l.0	-0.00005	-	-	0.00060	-	0.00033	0.00062	0.00038
'.4	-0.00005	-	-	-	-	-	-	-
).4	-	-	-	-	-	-	-	-

LOAD DEFLECTION CURVES

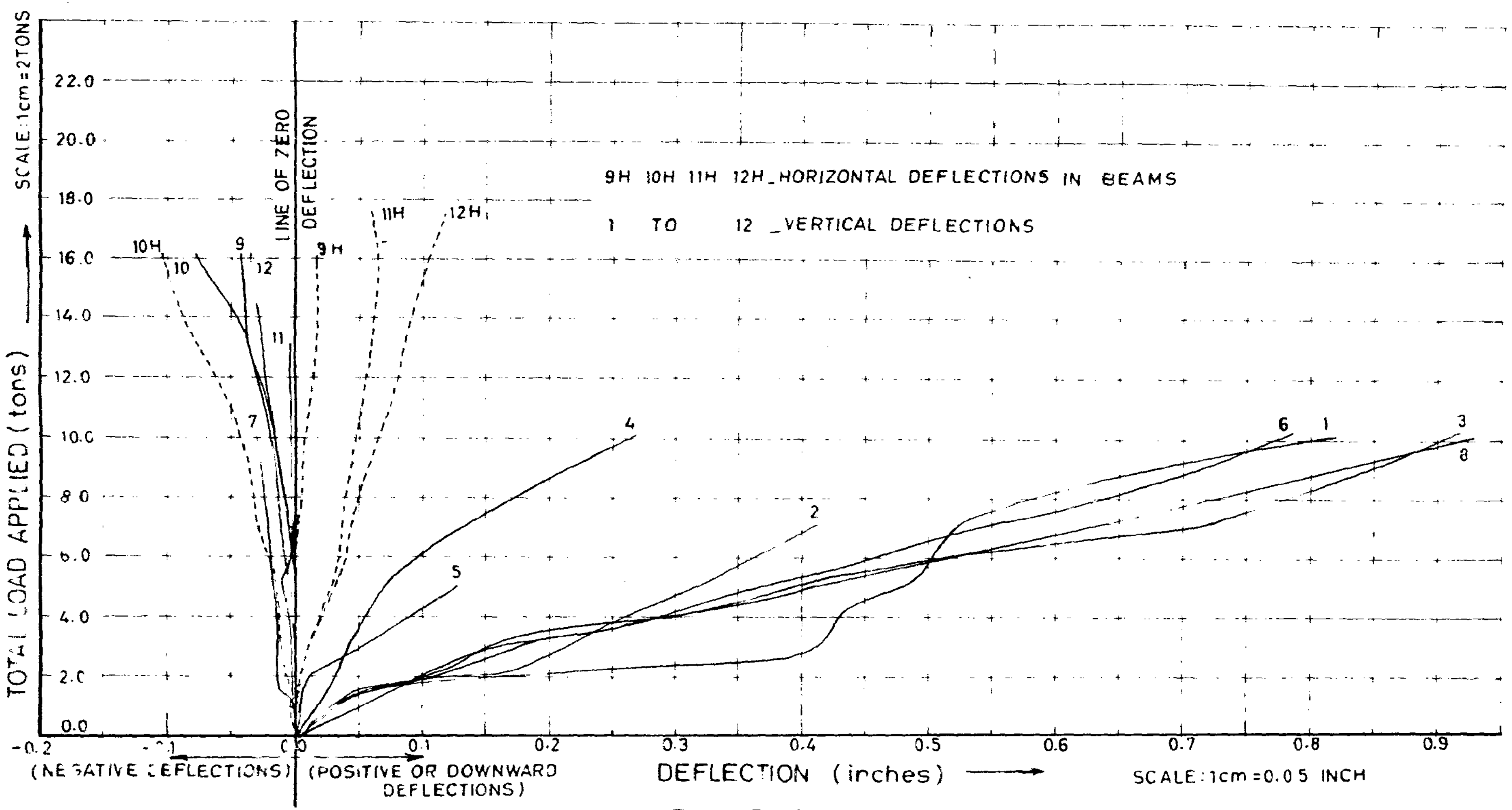

FIGURE_29

Bottom Surface Cracks

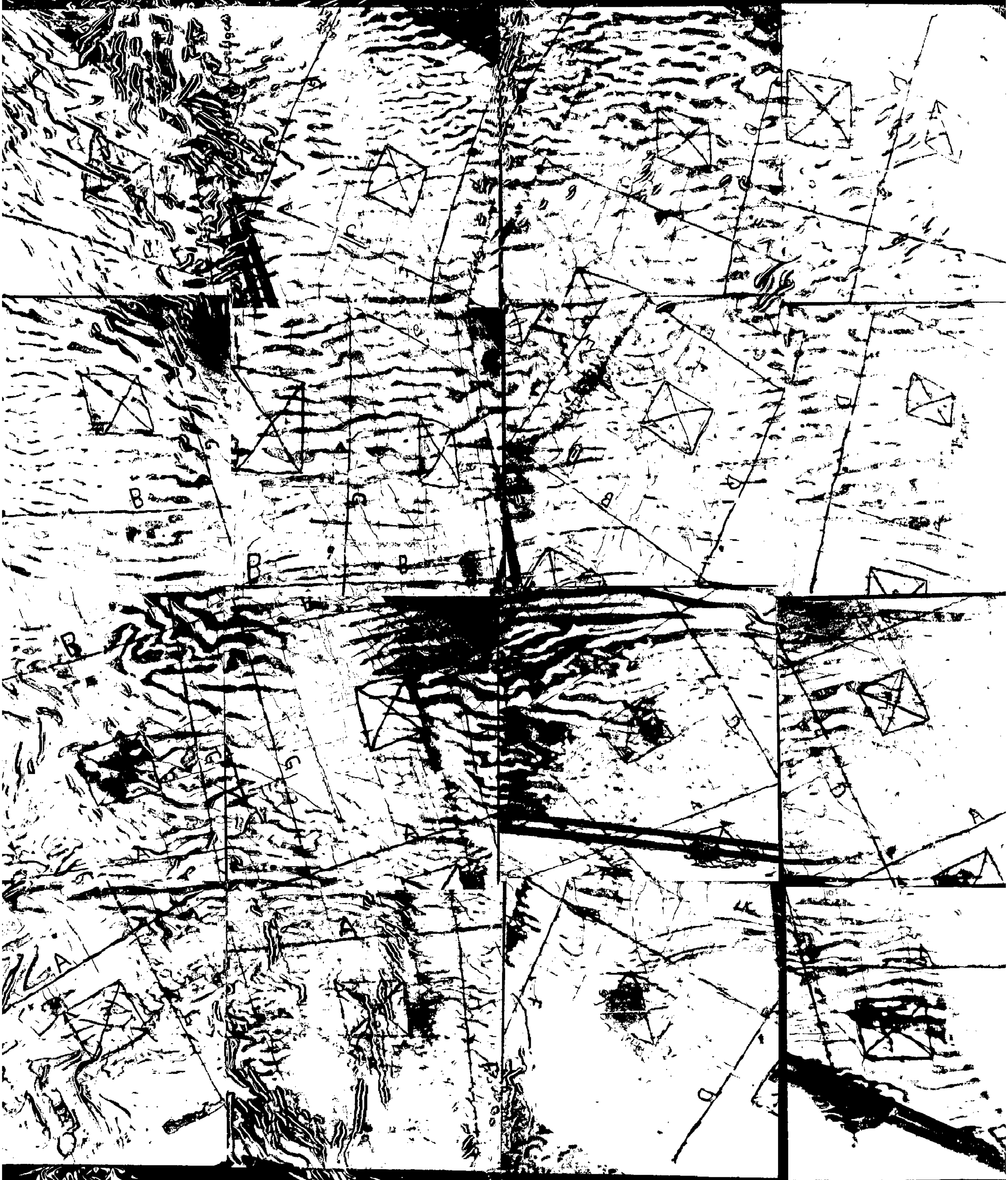

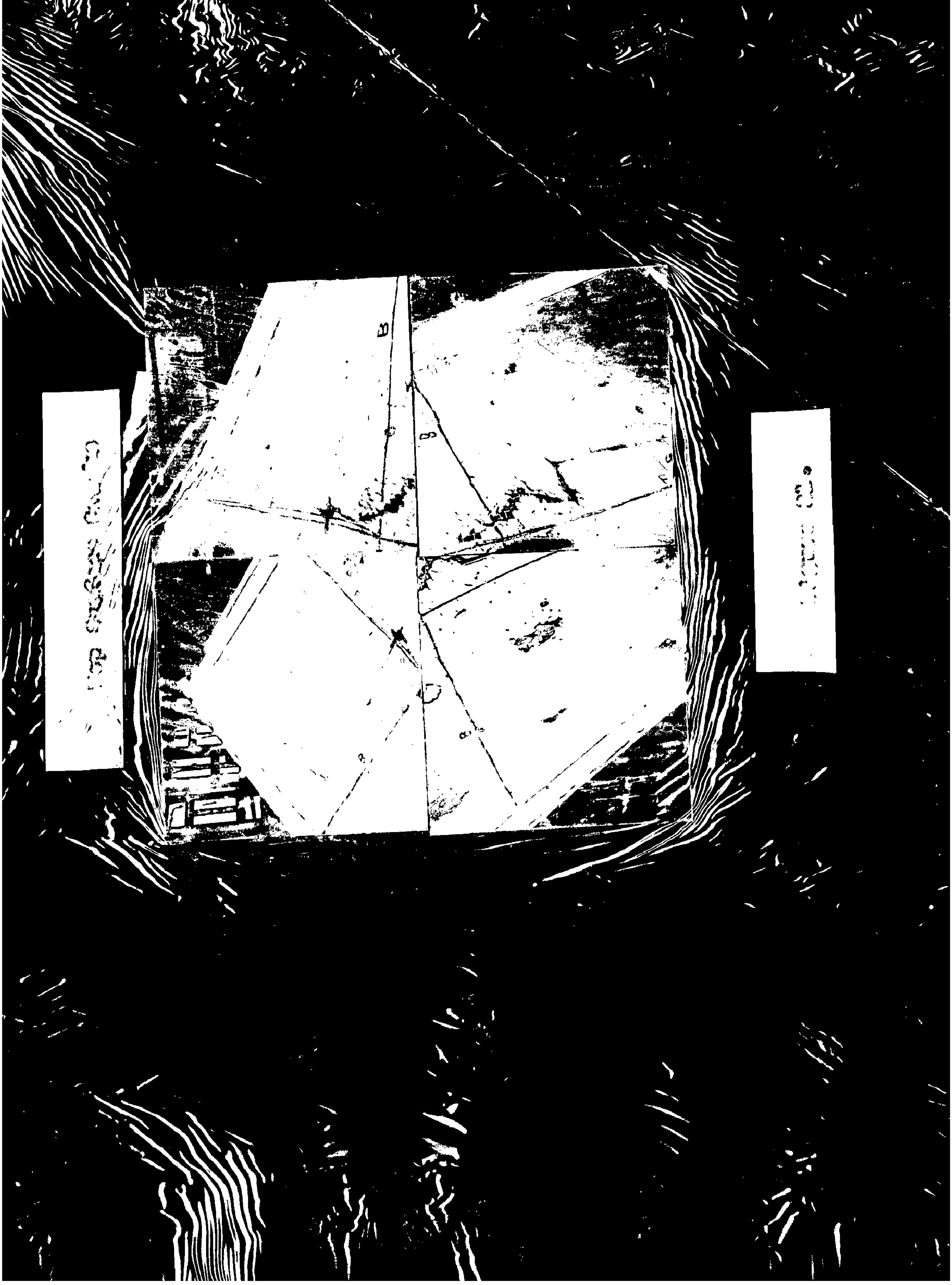

CRACK PATTERN OF THE BOTTOM SURFACE (IN PLAN)

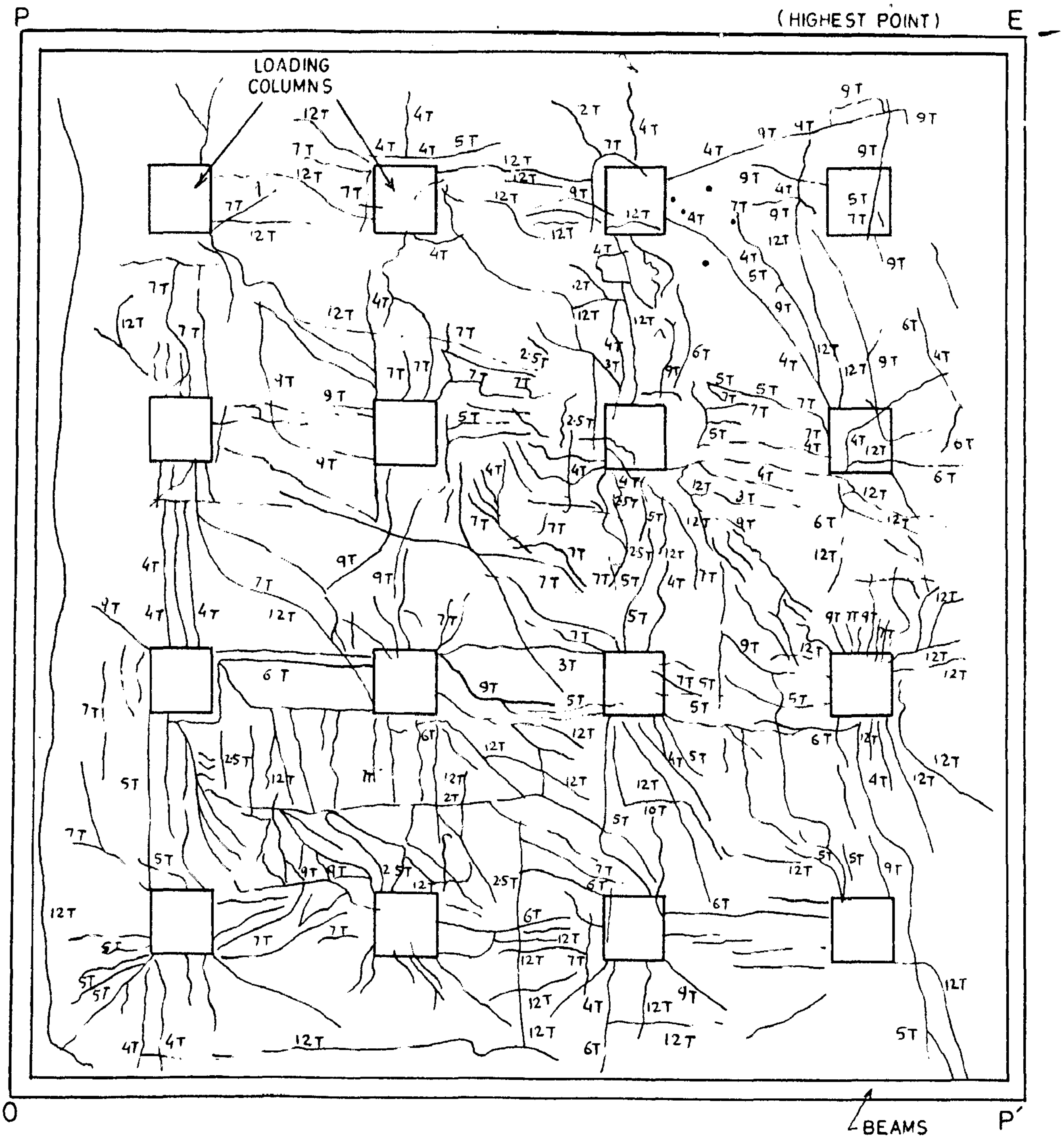

FIGURE_32

CRACK_PATTERN OF THE TOP SURFACE (IN PLAN)

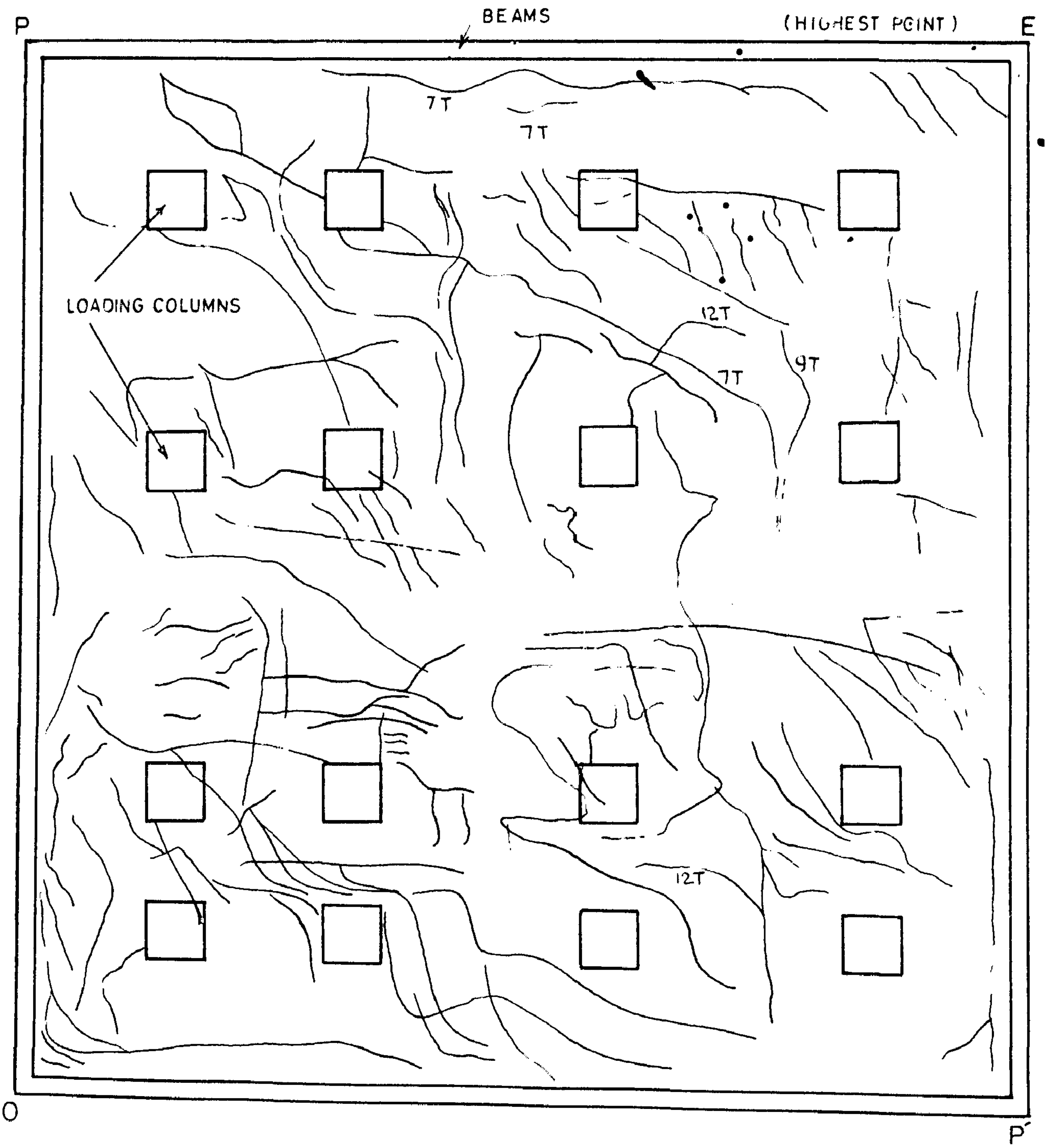

FIGURE_33

divided into sixteen parts for convenience of taking photographs, since the space below was too small. Due to curvature the scale is not the same, however, as some overlapping on all sides is available, a judgement can be made of the travel of the cracks. (Figure No.30). Photographs of the cracks at the top have been taken in four parts (Figure No.31). A general idea of crack patterns can be had from the Figure Nos. 32 and 33, which have been sketched by judgement.

In general, the cracks at the bottom were concentrated and emanated from the loading column-lines in both directions while at the top, the cracks appeared in the spaces between columns. Thus, there was local sagging under loading columns and the space between them was hogging up. Towards failure the boundaries of the columns became distinct at the bottom i.e. they were punching through the shell and deflections at the locations were comparatively larger. However, the dial-gauges were slightly away from the boundaries and so the results are expected to have been less affected by these local actions. The cracks at these places became wider and wider, more so towards the central region of the shell, till failure occurred, when no further load could be borne by the shell. The failure occurred at a load of

10.4 tons i.e. at 4.3 times the design load.

The shell remained in tact after failure, though some lifting of the pedastal at the highest point was observed over the brick column.

4.6. Discussion of Results.

Buckling-

The load-deflection curves are practically linear right-upto the failure and the deflections did not go beyond one inch in any case in the shell-model of considerably large dimensions. Except for the punching effects towards the ultimate load, even large localised deflections were not noticed anywhere, hence it could safely be said that the shell did not show any buckling behaviour. The failure of the shell was by yielding and punching combined.

Comparing the ultimate load with the buckling loads predicted by various investigators , it can be seen that the buckling loads given by Schmidt's and Csonka's analyses under-estimated the strength. This result has, however, to be viewed in the light of the modification of shell stiffness properties because of the attachment of loading columns with the shell surface.

Mode of Failure.

The failure was purely local on account of the concentrated load effects induced by the loading columns. The load distribution could not be feasible in a small thickness of $\frac{7}{16}$ inch. and columns under load tended to punch through the shell thickness. It could be expected, therefore, that if the load could be applied actually uniformly distributed, the load-factor would have been much higher than that obtained as 4.3.

Verification of Theories from Strain Observations.

The strain observations at the points 1,2,3,9 and 11 on the shell will be compared with the theoretical values as given by the membrane analysis and Vreedenburgh's edge moments for the working load.

Calculations of Strains.

Rotating x and y axes by 45^0 anticlockwise to obtain x' and y', we have as before (Articles 3.3 and 3.5)

$$x' = \frac{x + y}{\sqrt{2}} \; ; \quad y' = \frac{y - x}{\sqrt{2}}$$

Equation to the shell becomes,

$$z' = 0.00312\,(x'^2 - y'^2) - 0.252x'$$

$$\frac{dz'}{dx'} = 0.00624x' - 0.262 \text{ and } \frac{d^2z'}{dx'^2} = 0.00624$$

$$\frac{dz'}{dy''} = -0.00624y' \text{ and } \frac{d^2z'}{dy'^2} = -0.00624$$

$$k_1 = \frac{\dfrac{d^2z'}{dx'^2}}{\left[1 + \left(\dfrac{dz'}{dx'}\right)^2\right]^{3/2}}$$

$$\text{and } k_2 = \frac{\dfrac{d^2z'}{dy'^2}}{\left[1 + \left(\dfrac{dz'}{dy'}\right)^2\right]^{3/2}}$$

$$\lambda = \frac{0.76\sqrt{t}}{\sqrt[4]{k_1^2 + k_2^2}}$$

where k_1 and k_2 are principal curvatures at the edge point

p = 70 p.s.f.

t = 0.5 ft.

$\therefore 0.76\sqrt{t} = 0.537$

Values of moments will be taken from the Vreedenburgh's curve (16)

In the thickened section (vide Article 3.2); Moment of Inertia of equivalent concrete-section, $I = 253.4 \text{ in}^4$

Area of equivalent concrete section $A = 84.4 \text{ in}^2$

Distance of top fibre from the neutral axis, $h = 2.82$ ins.

For direct stresses,

$$p = 0.00624\ y - 0.1786$$

$$q = 0.00624\ x - 0.1786$$

$$N_x = -p_0 \times \frac{x}{2} \times p$$

$$N_y = -p_0 \times \frac{y}{2} \times q$$

$$S_y = N_y \sqrt{\frac{1 + q^2}{1 + p^2}} \quad \text{and} \quad S_x = N_x \sqrt{\frac{1 + p^2}{1 + q^2}}$$

The strains will be $\frac{Sx}{AE}$ or $\frac{Sy}{AE}$ as the case be.

(I) <u>Point No.1 (14,14)</u>

Corresponding edge point = (14,0)

$$\therefore x' = \frac{14}{\sqrt{2}} = 9.9 \quad \text{and} \quad y' = -9.9$$

$$\frac{dz'}{dx'} = 0.0616 - 0.252 = -0.1904$$

$$\frac{dz'}{dy'} = -0.0616$$

$$\therefore \quad k_1 = \frac{0.00624}{\left[1+0.03628\right]^{3/2}} = 0.00594$$

$$k_2 = -\frac{0.00624}{[1+0.0038]^{3/2}} = -.00622$$

$$\lambda = \frac{0.75 \times 0.707}{\sqrt[4]{(0.351+0.387)\times10^{-4}}} = 5.79 \text{ ft.}$$

$$\frac{14.4}{\lambda}\times\frac{4}{\pi} = 3.09$$

$$\therefore \text{ B.M.} \approx + 0.1\, p_o \lambda^2 = 7 \times 5.79^2 \times 12$$

$$= 2920 \text{ lbs.in/ft.}$$

$$\text{Top strain (compressive)} = \frac{M\ h}{I\ E} = \frac{2920 \times 2.82}{253.4\times2.14\times10^6}$$

$$= 14.68\times10^{-6}$$

For the direct stress,

$$p = 0.00624y - 0.1786 = -0.09124$$

$$q = 0.00624x - 0.1786 = -0.09124$$

$$N_y = -p_o \times \frac{y}{2} \times (0.00624x - 0.1786) = 44.2 \text{ lbs/ft.}$$

$$\therefore S_y = N_y\sqrt{\frac{1+q^2}{1+p^2}} = 44.2 \text{ lbs/ft.}$$

$$\therefore \text{ Strain} = \frac{S_y}{A\ E} = \frac{44.2}{84.4 \times 10^6 \times 2.14}$$

$$= 2.45 \times 10^{-7} \text{ (tensile)}$$

Resultant strain at top fibre

$= (146.8 - 2.45) \times 10^{-7}$

$= 0.0000144$ (compressive).

(II) Point No.2 (56,14)

Corresponding edge point $= (56,0)$.

$\therefore x' = 39.6$ and $y' = -39.6$

$\frac{dz'}{dx'} = -0.005$

$\frac{dz'}{dy'} = -0.247$

$k_1 = 0.00624$

$k_2 = -0.0057$

$$\lambda = \frac{0.76 \times 0.707}{\sqrt[4]{(0.39+0.325)\times10^{-4}}}$$

$= 5.84$ ft.

$\frac{14}{\lambda} \times \frac{4}{\pi} = 3.06$

$\therefore$ B.M. $\approx + 0.1\, p_o \lambda^2 = 7 \times 5.84^2 \times 12$

$= 2860$ lb.in/ft.

Top strain(compressive) $= \frac{2860 \times 2.82}{253.4 \times 2.14\times10^6}$

$= 14.78\times10^{-6}$

For direct stress,

$p = -0.09124, \quad q = 0.1709$

$N_y = -837$ lb/ft. $\quad S_y = -860$ lb./ft.

$\therefore$ Strain $= \dfrac{S_y}{A\ E}$

$$= -\frac{860}{84.4 \times 2.14 \times 10^6}$$

$= 4.77 \times 10^{-6}$ (compressive)

$\therefore$ Resultant strain at top fibre

$= (14.78 + 4.77) \times 10^{-6}$

$= 0.0000196$ (compressive)

(III) <u>Point No.3.(98,14)</u>

Corresponding edge point = (98,0)

$x' = \dfrac{98}{\sqrt{2}} = 69.3$ and $y' = -69.3$

$\dfrac{dz'}{dx'} = 0.180$

$\dfrac{dz'}{dy'} = -0.432$

$k_1 = 5.94 \times 10^{-3}$

$k_2 = -4.83 \times 10^{-3}$

$$\therefore \lambda = \frac{0.76 \times 0.707}{\sqrt[4]{0.351 + 0.233 \times 10^{-1}}} \quad \therefore = 6.14 \text{ ft.}$$

$$\therefore \frac{14}{\lambda} \times \frac{4}{\pi} = 2.91$$

$$B.M. \approx + 0.1\, p_o \lambda^2 = 7 \times 6.14^2 \times 12$$

$$= 3170 \text{ lbs.in/ft.}$$

$$\text{Total strain (compressive)} = \frac{3170 \times 2.82}{253.4 \times 2.14 \times 10^6}$$

$$= 16.5 \times 10^{-6}$$

For direct stress,

$p = -0.09124$ and $q = 0.4204$

$N_y = -20.6$ lb/ft. and $S_y = -22.3$ lb/ft.

$$\therefore \text{Strain} = \frac{S_y}{A \times E} = -\frac{22.3}{84.4 \times 2.14 \times 10^6}$$

$$= -1.237 \times 10^{-7}$$

(compressive)

$\therefore$ Resultant strain at top fibre

$= (16.5 + 0.1237) \times 10^{-6} = -0.0000166$

(IV) <u>Point No.9 (112, 14)</u>

The point is on the edge itself.

$$x' = \frac{112 + 14}{\sqrt{2}} = 89 \; ; \; y' = \frac{14 - 112}{\sqrt{2}}$$

$$= -69.4$$

$$\frac{dz'}{dx'} = 0.303$$

$$\frac{dz'}{dy'} = -0.433$$

$$k_1 = 0.00546$$

$$k_2 = -0.00484$$

$$\lambda = \frac{0.76 \times 0.707}{\sqrt[4]{0.298+0.234\times10^{-1}}} = 6.28 \text{ ft.}$$

$$\therefore \text{B.M.} = -0.5 \, p_o \lambda^2 = -35\times6.28^2\times12$$

$$= -16600 \text{ lb.in/ft.}$$

$$\text{Top strain} = \frac{16600 \times 2.82}{253.4 \times 2.14\times10^6}$$

$$= 86.4 \times 10^{-6} \text{ (tensile)}$$

For direct stress,

$$p = -0.0912 \; , \; q = 0.5204$$

$$N_x = 358 \text{ lb/ft. and } S_x = 316.2 \text{ lb/ft.}$$

$$\text{Strain} = \frac{S_x}{A \times E} = 1.755 \times 10^{-6} \text{ (tensile)}$$

$\therefore$ Resultant strain $= 86.4 \times 10^{-6} + 1.755 \times 10^{6}$

$= 0.000088$ (tensile)

(V) Point No.11 (56,0)

The point is on the edge itself

$$x' = \frac{56}{\sqrt{2}} = 39.6 \text{ and } y' = -39.6$$

$$\frac{dz'}{dx'} = -0.005$$

$$\frac{dz'}{dy'} = -0.247$$

$$k_1 = 0.00624$$

$$k_2 = -0.00573$$

$$= \frac{0.76 \times 0.707}{4\sqrt{0.39 + 0.327 \times 10^{-1}}}$$

$= 5.84$ ft.

B.M. $= -35 \times 5.84^2 \times 12 = -14280$ lb.in/ft.

Strain on the top fibre $= \dfrac{14280 \times 2.82}{253.4 \times 2.14 \times 10^6}$

$= 74.4 \times 10^{-6}$ (tensile)

For direct stress,

Since $N_y = 0$, $S_y = 0$ and therefore strain is zero.

∴ Resultant strain = 0.000074 (tensile)

The results can be tabulated as below:

Table No.12

Point Nos. / Strains	1	2	3	9	11
Calculated	-0.0000144	-0.0000196	-0.0000166	+0.000088	+0.00007
Observed	-0.0000145	-0.000027	-0.000055	+0.000075	+0.00003

The strains are of the same order and sign. In magnitude they are quite close except for the point No.3, which shows that the membrane analysis and the relations given by Vreedenburgh hold well at least within the working range of the load. The strains are varying almost linearly in this range as it should be within the elastic range(Fig.No.34

LOAD_STRAIN CURVES IN CONCRETE

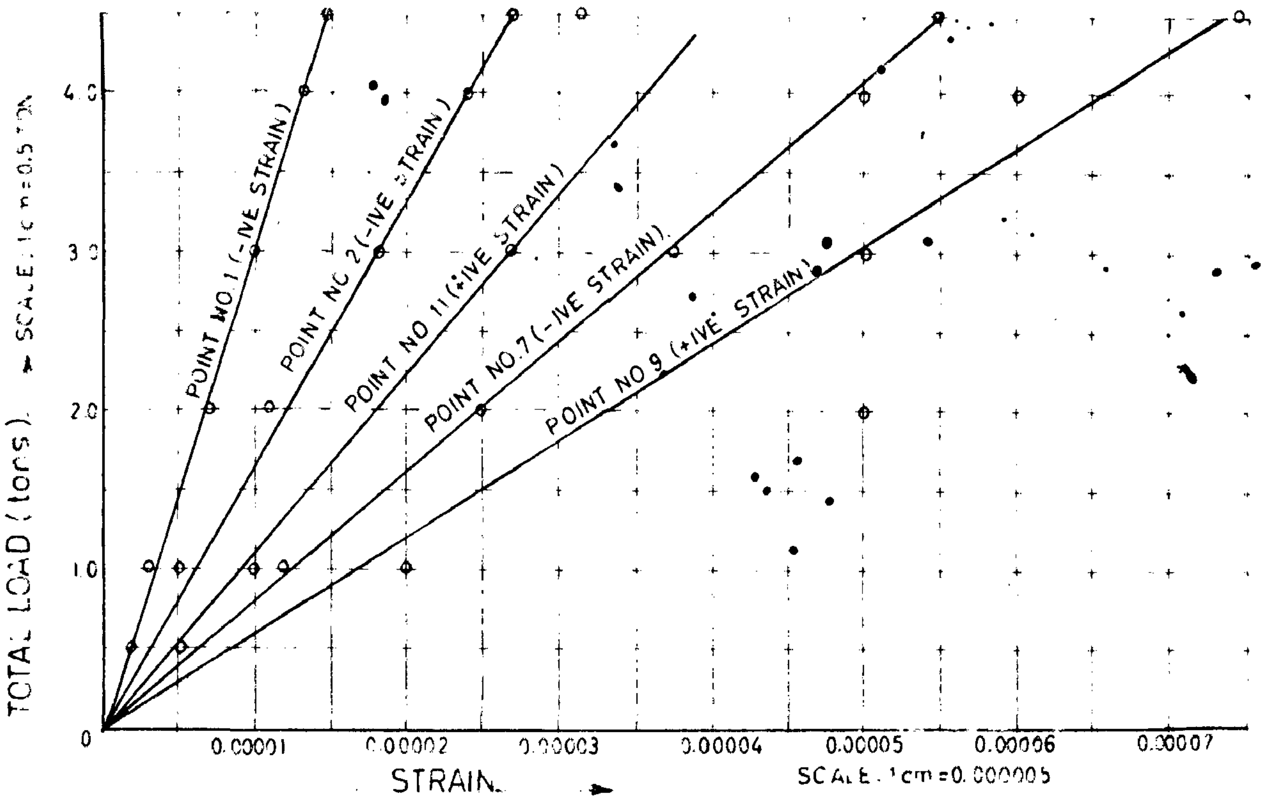

FIGURE_34

LOAD_STRAIN CURVES IN TIE BARS

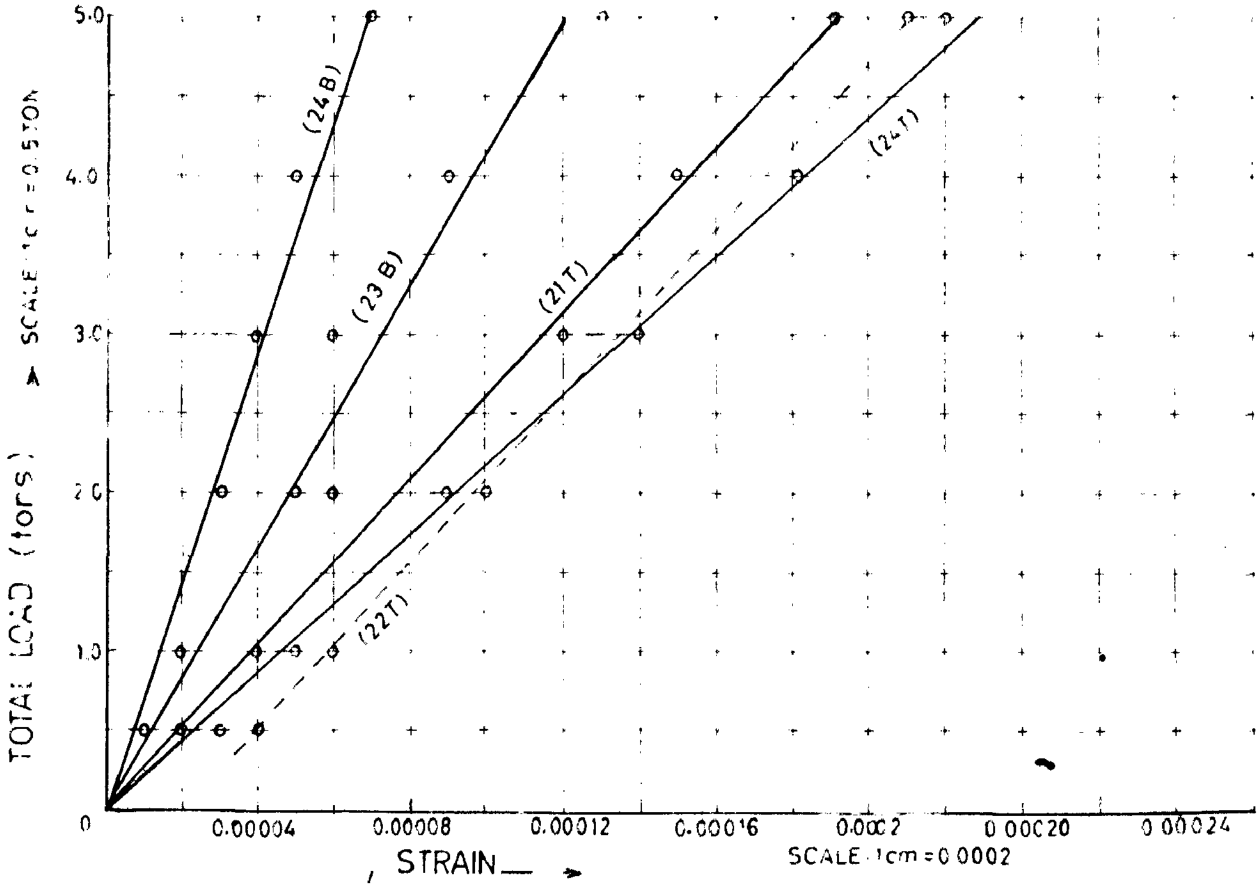

FIGURE_35

The strains measured on the reinforcement in the beams are, however, irregular.

Strains in Tie-bars.

For the four tie bars of 1 in. diameter in the shell model, if the total tensile force be P,

$$\text{Stress} = \frac{P}{4 \times A}, \text{ where } A \text{ is the cross-sectional area of all bars.}$$

$$= \frac{P}{\pi}$$

$$\therefore \quad \text{Strain} = \frac{P}{\pi \times 30 \times 10^6}$$

$$P \text{ in Prototype} = 1.85 \times 10^6 \text{ lbs.}$$

$$\therefore \text{ P in model} = \frac{1.85 \times 10^6}{9.33^2} \text{ p.s.i.}$$

$$\therefore \text{ Strain in model ties} = 0.00022$$

Strains as observed are as below at the working load of 4.5 tons.

Table No.13

Points	21T	22T	23B	24T	24B
Strains	0.00017	0.00020	0.00011	0.00020	0.0006

We observe a close proximity of these values with the calculated ones. The order is the same and at three points the values are very close. The greater difference lies at those points , where strain gauges were pasted at bottom and it is quite likely that full strain could not be transferred there due to imperfect pasting of the gauges. Again the strains upto this load are varying linearly proving the accuracy in the elastic range (Figure No.25).

Model Analysis and Model Test.

Further, it can be said that the model analysis and model test imparted a fairly good idea of the stress strain conditions in the proto-type, since all calculations for the theoretical values have been based on the prototype design and compared with the observations in the model, which have tallied satisfactorily.

CHAPTER 5

CONCLUSION

The following conclusions are drawn from the experiment:-

(i) The buckling strength of hyperbolic paraboloids is expected to be high and the values predicted by Csonka or Schmidt for synclastic shells are far too conservative when applied to anticlastic shells. It is possible that the simple double curvature formula $p_{cr} = \propto \frac{Et^2}{r_1 r_2}$ may not hold good at all in the case of anticlastic shells. The shell rise to span ratio may be too important to be neglected.

(ii) The ultimate strength of such shells also appears to be high. Inspite of many adverse conditions (thinness of slab, concentration of loads causing punching) the load-factor is 4.3. Hence much higher load-factor may be available.

(iii) The membrane analysis and the approximate edge moment relations given by Vreedenburgh seem to give fairly good and accurate values at least within the working range.

(iv) The linearity in the elastic range holds good in the shell concrete and tie bars.

(v) The model test of the R.C. hyperbolic paraboloid shell represents a satisfactorily true picture of the values estimated in the design of the proto-type at least in the elastic range.

REFERENCES

1. Wansleben's Theory-	K. Girkman, Flachentragwerke, Springer Vienna, 4th Edition, 1956 pp. 516-529.
2. Richard R. Bradshaw-	"Some Aspects of Concrete Shell Buckling". A.C.I. Journal March 1963 Proceedings Vol.60, No.3.
3. Timoshenko and Gere.	"Theory of Inelastic Stability." 1961 Edition. p 443.
4. H. Schmidt (Dresden)-	"Proceedings of the Symposium on Shell Research, Delft, Aug. 30 to Sept. 2, '64. pp.161-181.
5. Ibid.	Discussion on the paper in (4).
6. P. Csonka-	"The Buckling of a Spheroidal Shell Curved in Two Directions", Acta Technica, Academiae Scientarium Hungaricae, Budapest, Tomus XIV, 1956.
7. Eric Reissner (Associate Prof. M.I.T)	"On Some Aspects of The Theory of Thin Elastic Shells". (J. Boston Society of Civil Engineers) pp. 42-100 (1955)
8. K. Marguerre-	Zur Theorie Der Gekrummten Platte Grosser Formanderung, Proc. 5th Int. Congress Appl. Mech. pp. 93-101 (1938)
9. Anthony Ralston-	"On the Problem of Buckling of a Hyperbolic Paraboloid Shell by Its Own Weight", J. Maths and Physics Apr. 1956.
10. Nicolas Esquillon, (France.)	"The Design and Construction of the Shell Roof of the Exhibition Palace of the Noliond Centre of Industries and Technology, Paris" (Cement and Concrete Association Publication)

11. Dr. A.L.Parme- "Elementary Analysis of Hyperbolic Paraboloid Shells" I.A.S.S. Bulletin No.4. 1960.

12. Mario G.Salvadori-. "Discussion pp. 1018-1021" on paper "Shells of Double Curvature" by Dr. A.L.Parme in A.S.C.E.T 123 (1958). Also A.S.C.E. P 1057 (1956)

13. IA.S.S. Bulletin No.2.

14. A.L.Bouma and A.M.Haas. General Report in "Symposium on Shell Research" Delft.(Aug.20-Sept.2, '61) (I.A.S.S. Bulletin No.11).

15. Kriz. Discussion on paper "Experimental Studies of H.P. Structures under Static and Dynamic Loads," By Prof. J. Brennan P.C .E., Syracuse University in "Proceedings of the Symposium on Shell Research" Delft. (Aug.30-Sept. 2, 1961)

16. C.G.J.Vreedenburgh- Phillips Technical Review Vol.20, No.1, 1958-59. pp.9-27 "The Hyperbolic Paraboloid Shell and its Mechanical Properties."

17. Pasala Dayaratnam, Andhra 'Varsity and Kurt H.Gerstle, Colorado. "Buckling of Hyperbolic Paraboloids" in Proceedings of the World Conference on Shell Structures, Oct-1-4, 1962, Sanfransisco, California pp. 289-296 (Published in 1964).

18. Portland Cement - Association. "Elementary Analysis of Hyperbolic Paraboloid Shells" R/C 35,1960.

19. A.Pflueger- "Stabilitaets Probleme Der Elastostatik" Springer Verlag,1950.

20. S.P.Timoshenko and J.M.Gere. "Theory of Elastic Stability, McGraw Hill 1961, pp. 337.

21. R.E.Rowe "Tests on Four Types of Hyperbolic Shells", Proc. of the Symposium on Shell Research Delft, 1961, pp.16-35.

22. H.H.Bleich and M.G.Salvadori - "Bending Moments on Shell Boundaries" Journal Struct. Div. A.S.C.E. 1959.

23. A.P.Agarwal- M.E. Dissertation (1962), University of Roorkee on "Study of a Large Doubly Curved Shell Roof".

24. Dr. Jai Krishna and- Dr. O.P.Jain. R.C.C. Vol. II pp. 33.

25. Engineering News Record, May 19th Issue of 1962.

26. Engineering News Record, March 1962.